

SLOW-FAST SYSTEM IN ROSALES-MAJDA COMBUSTION MODEL WITH FRACTIONAL ORDER KINETICS

CLAUDE-MICHEL BRAUNER, JINLONG JING, AND ROBERT ROUSSARIE

ABSTRACT. We consider traveling wave solutions of a one-dimensional model for detonation waves derived by Rosales and Majda, when the reaction order α belongs to $[0, 1)$. The chemical kinetics is a simplified Arrhenius law or a Heaviside function. The model in the reaction zone is a slow-fast dynamical system for a vector representing temperature and mass fraction, which depends on the velocity c and small viscosity β . Our goal in this paper is to study the bifurcation diagram in the (β, c) parameter space and identify the nature of the trajectories corresponding to viscous shock waves. The demonstrations are based on a variety of techniques including the Poincaré-Bendixson theorem and the Fenichel theory. Theoretical results are confirmed by numerical computations.

Dedicated to Roger Temam on his 85th Birthday, with Respect and Admiration.

1. INTRODUCTION

In this paper, we consider the one-dimensional model derived by Rosales and Majda (see [24]) for studying detonation waves when the wave velocity approaches the speed of sound, in the wake of the famous “Majda model” introduced in 1981 by Andrew Majda (see [6, 18, 19]). More specifically, according to [17, 25], we will study a range of models where the order of the chemical reaction, denoted by α , lies between 0 and 1 (see [3] for a similar problem). The original model proposed by Rosales and Majda corresponds to $\alpha = 1$, see [24, 26].

In dimensionless variables, the Rosales–Majda model with fractional reaction order $0 \leq \alpha < 1$ is expressed as follows:

$$(1.1) \quad \begin{cases} T_t + \left(\frac{T^2}{2} - q_0 Z\right)_x = \beta T_{xx}, \\ Z_x = K \varphi(T) Z^\alpha, \\ \lim_{x \rightarrow +\infty} Z(x, t) = 1. \end{cases}$$

In the system (1.1), $x \in \mathbb{R}$ and $t > 0$ are the space and time variables, respectively, $T(x, t)$ is a lumped variable representing the temperature, $Z(x, t)$ is the mass fraction such that $0 \leq Z(x, t) \leq 1$. Furthermore, $q_0 > 0$ is the heat release, $\beta > 0$ is the (small) viscosity and $K > 0$ is the reaction rate, $\varphi(T)$ stands for the chemical kinetics.

Our aim is to study the existence of traveling wave solutions $T(\xi)$, $\xi = x - ct$, of system (1.1) propagating at a velocity $c > 0$ and connecting two equilibria T_- and T_+ such that $T_+ < T_i < T_-$ where T_i is the ignition temperature. The structure of a solution is a *traveling reactive shock wave*, namely a viscous shock followed by a reaction zone that ends when Z vanishes. More precisely, assuming for convenience that T reaches the ignition temperature at $\xi = 0$, the real

2020 *Mathematics Subject Classification.* 35C07, 34E13, 34C05, 34A26, 80A25.

Key words and phrases. Traveling reactive shock waves, slow-fast differential systems, Poincaré-Bendixson theory, bifurcation diagram, free interface, combustion.

line will be divided into the shock wave region $\{\xi > 0\}$, the reaction zone $\{-\ell < \xi < 0\}$, and beyond, the region $\{\xi < -\ell\}$. Here, $\xi = -\ell$ is a finite *free interface* (see [3, 17]) defined by $Z(-\ell) = 0$. Obviously, the free interface is at $-\infty$ when $\alpha = 1$ as in [24, 26].

In this paper, in addition to the free interface, there are other significant differences from [24, 26]. We will reformulate the problem in the reaction region as a slow-fast system for small viscosity β , see Section 1.3. Moreover, in contrast to [24, 26], the heat release q_0 is a fixed parameter. Instead, we will search for a bifurcation diagram in the parameter space (β, c) , see Figure 1.

1.1. Formulation of the problem. We now take a closer look at the model (1.1). According to [24], the chemical kinetics is an ignition temperature kinetics of the Arrhenius type. In the following we assume that the ignition temperature T_i is a real number such that (see [17])

$$(1.2) \quad 0 < T_i < \sqrt{2q_0}.$$

For simplicity, we assume also that φ is discontinuous at the ignition temperature T_i , $\varphi(T) = 0$ for $T \in [0, T_i)$, and is sufficiently smooth and positive whenever for $T \geq T_i$. There will be an additional technical hypothesis for large T , see below. In this paper, the following two examples of functions φ are considered:

- (i) the Heaviside $\varphi(T) = H(T - T_i)$;
- (ii) a simplified form of the Arrhenius law that reads (see also [13, 14])

$$(1.3) \quad \varphi(T) = H(T - T_i) \exp\left(-\frac{T_a}{T}\right),$$

where $T_a = E_a/R > 0$, where E_a is the activation energy and R is the gas constant (see, e.g., [4, Section 1.3]). Obviously, case (i) corresponds to the limit case $T_a = 0$, so the Heaviside function can be regarded as a simplification of the Arrhenius law.

For given $K, q_0 > 0$, $0 \leq \alpha < 1$, we seek a traveling wave solution $(T(x - ct), Z(x - ct))$, propagating from the left to right with velocity $c > 0$ to be determined. In the coordinate $\xi = x - ct$, we search for $T(\xi)$ and $Z(\xi)$, continuously differentiable and continuous functions, respectively, solutions of

$$(1.4) \quad \begin{cases} -cT_\xi + \left(\frac{T^2}{2} - q_0Z\right)_\xi = \beta T_{\xi\xi}, \\ Z_\xi = K\varphi(T)Z^\alpha. \end{cases}$$

with conditions at infinity as follows:

$$(1.5) \quad \begin{cases} \lim_{\xi \rightarrow +\infty} T(\xi) = T_+, & \lim_{\xi \rightarrow +\infty} Z(\xi) = 1, \\ \lim_{\xi \rightarrow -\infty} T(\xi) = T_-, \end{cases}$$

where T_- and T_+ are such that $T_+ < T_i < T_-$.

Integration of (1.4) yields

$$(1.6) \quad \begin{cases} \beta T_\xi = -cT + \frac{T^2}{2} - q_0Z + A, \\ Z_\xi = K\varphi(T)Z^\alpha. \end{cases}$$

where A is a constant. Throughout this paper, for simplicity, we choose $T_+ = 0$; hence, $A = q_0$ and the differential system reads as follows:

$$(1.7) \quad \begin{cases} \beta T_\xi = -cT + \frac{T^2}{2} + q_0(1 - Z), \\ Z_\xi = K\varphi(T)Z^\alpha, \end{cases}$$

with conditions (1.5) at infinity.

Moreover, taking advantage of the translation invariance, we fix

$$(1.8) \quad T(0) = T_i,$$

and seek a solution which verifies

$$(1.9) \quad T(\xi) < T_i \text{ when } \xi > 0, \quad T(\xi) > T_i \text{ when } \xi < 0,$$

hence, $T_- = \lim_{\xi \rightarrow -\infty} T(\xi) > T_i$.

As we mentioned above, there are the following three regions, keeping in mind that $T \in C^1(\mathbb{R})$, $Z \in C^0(\mathbb{R})$:

(i) The shock wave region $\{\xi > 0\}$: because $T(\xi) < T_i$, it holds $\varphi(\xi) = 0$, therefore $Z(\xi) = 1$ whenever $\xi > 0$. The system (1.7) for (T, Z) reads simply in the shock wave region:

$$(1.10) \quad \begin{cases} \beta T_\xi = -cT + \frac{T^2}{2}, \\ Z \equiv 1, \\ T(0) = T_i, \quad \lim_{\xi \rightarrow +\infty} T(\xi) = 0. \end{cases}$$

(ii) The reaction zone $\{-\ell < \xi < 0\}$. The quantity $-\ell$, $\ell > 0$, is a free interface that we may also call the *trailing interface* by analogy with [2, 3], defined by

$$(1.11) \quad -\ell = \inf \{\xi < 0, Z(\xi) > 0\}.$$

Consider the case where $\varphi(T) = H(T - T_i)$: because $T > T_i$ it holds $\varphi(T) = 1$ when $\xi < 0$, hence $Z_\xi = KZ^\alpha$ for $\xi < 0$ with $Z(0) = 1$. Then,

$$\ell = \frac{1}{K(1 - \alpha)}, \quad 0 \leq \alpha < 1,$$

that is, $\ell < +\infty$ (see [17]).

Therefore, we anticipate that, whenever $0 \leq \alpha < 1$, the reaction zone is finite and the system (1.7) for (T, Z) reads

$$(1.12) \quad \begin{cases} \beta T_\xi = -cT + \frac{T^2}{2} + q_0(1 - Z), \\ Z_\xi = K\varphi(T)Z^\alpha, \\ T(0) = T_i, \quad Z(0) = 1, \end{cases}$$

and the condition $Z(-\ell) = 0$ which determines ℓ and provides the value of $T(-\ell)$.

(iii) In the region $\{\xi < -\ell\}$ following the finite reaction zone, the system (1.7) for (T, Z) reads:

$$(1.13) \quad \begin{cases} \beta T_\xi = -cT + \frac{T^2}{2} + q_0, \\ Z \equiv 0, \\ \lim_{\xi \rightarrow -\infty} T(\xi) = T_-. \end{cases}$$

The candidates for T_- are $T_0(c) = c + \sqrt{c^2 - 2q_0}$ and $T_1(c) = c - \sqrt{c^2 - 2q_0}$ with the condition $c \geq \sqrt{2q_0}$. By analogy with detonations (see [24]), the equilibria $(T_0(c), 0)$ and $(T_1(c), 0)$ correspond, respectively, to a *strong reactive wave* and a *weak reactive wave*.

Definition 1.1. *Again by analogy, the minimal value $c = \sqrt{2q_0}$ is called the Chapman-Jouguet (CJ) velocity and will be denoted by c^{cj} throughout the paper.*

We observe that $T_0(c) \geq c \geq c^{cj} > T_i$ (see (1.2)) and also $T_1(c) > 0$. For $c \rightarrow +\infty$ we have that $T_0(c) \rightarrow +\infty$ and $T_1(c) \rightarrow 0_+$ (more precisely, $T_1(c) \sim q_0/c^2$).

1.2. Background results. In contrast with [24, 26], we consider system (1.10)–(1.13) at fixed $q_0 > 0$ and look for traveling wave solutions $(T(\xi), Z(\xi)) \in C^1(\mathbb{R}) \times C^0(\mathbb{R})$ which travel at speed $c \geq c^{cj}$. Trajectories which connect equilibria $(T_0(c), 0)$, $(T_1(c), 0)$, $(\sqrt{2q_0}, 0)$ to the equilibrium state $(T_+, 1)$ correspond, respectively, to strong reactive solutions, weak reactive solutions, Chapman-Jouguet reactive solutions.

More specifically, when $c > c^{cj}$, there are three types of strong reactive traveling waves such that $T_- = T_0(c)$:

- (i) monotonic solutions such that $T(\xi) \rightarrow T_0(c)$ exponentially when $\xi \rightarrow -\infty$;
- (ii) non-monotonic solutions with a bump (a combustion spike), in the reaction zone such that $T(\xi) \rightarrow T_0(c)$ exponentially when $\xi \rightarrow -\infty$;
- (iii) special solutions, or solutions of special type, such that $T \equiv T_0(c)$ beyond the finite reaction zone. We may also call them *finite time solutions* in the context of the slow-fast system and the “time” τ .

There are also weak reactive waves of special type such that $T_- = T_1(c)$ and $T \equiv T_1(c)$ beyond the finite reaction zone.

In the case $c = c^{cj}$, then $T_- = \sqrt{2q_0}$ and there are only two types of solutions, namely Chapman-Jouguet (CJ) solutions with a bump such that $T(\xi) \rightarrow \sqrt{2q_0}$ algebraically when $\xi \rightarrow -\infty$, and solutions of special type such that $T \equiv \sqrt{2q_0}$ beyond the finite reaction zone.

We summarize our results in the following theorems, with the notation

$$(1.14) \quad c_* = \frac{T_i^2 + 2q_0}{2T_i}.$$

As $T_i > 0$ and $q_0 > 0$, we have that $c_* > c^{cj}$. In the domain $(\beta > 0, c \geq c^{cj})$, it holds (see Figure 1):

Theorem 1.2. (i) *There exists a function $\beta_0(c) : [c^{cj}, +\infty) \rightarrow \mathbb{R}^+$, of class $[\frac{1}{1-\alpha}]$, such that there is a strong reactive solution of special type for $\beta = \beta_0(c)$;*

(ii) *there exists a function $\beta_1(c) : [c^{cj}, c_*) \rightarrow \mathbb{R}^+$, of class $[\frac{1}{1-\alpha}]$, such that there is a weak reactive solution of special type for $\beta = \beta_1(c)$;*

(iii) *the curves $\beta_0(c)$ and $\beta_1(c)$ enjoy the following properties:*

- (a) *for all $c > c^{cj}$, we have that $\beta_0(c) < \beta_1(c)$;*
- (b) *$\beta_0(c) \rightarrow +\infty$ as $c \rightarrow +\infty$;*
- (c) *$\beta_1'(c) > 0$ for $c \in (c^{cj}, c_*)$, moreover $\beta_1(c) \rightarrow +\infty$ when $c \rightarrow c_*$;*

(iv) *for $c > c^{cj}$, $0 < \beta < \beta_0(c)$, there is a strong reactive solution with a bump; for $\beta_0(c) < \beta < \beta_1(c)$, there is a strong reactive wave of monotonic type; finally, when $c^{cj} < c < c_*$ and $\beta \geq \beta_1(c)$, there is no solution.*

An important result is that the bifurcation diagram admits (at least) two critical points. The first one belongs to the axis $c = c^{cj}$.

Theorem 1.3. (Critical point (β^{cj}, c^{cj})). *It holds:*

- (i) for $c = c^{cj}$, there exists a unique $\beta^{cj} \in (0, +\infty)$ such that $\beta^{cj} = \beta_0(c^{cj}) = \beta_1(c^{cj})$;
- (ii) at the critical point (β^{cj}, c^{cj}) , there is a Chapman-Jouguet reactive wave of special type.
- (iii) the union of the graphs of β_0 and β_1 with the point (β^{cj}, c^{cj}) is a simple curve (B) in the parameter space, of class $[\frac{1}{1-\alpha}]$. The mapping $\tilde{c}: \beta \rightarrow c$ defined by the curve (B) locally around (β^{cj}, c^{cj}) has a quadratic minimum at β^{cj} , i.e., $\tilde{c}'(\beta^{cj}) = 0$, $\tilde{c}''(\beta^{cj}) > 0$;
- (iv) for $c = c^{cj}$, $\beta \in (0, \beta^{cj})$, there is a Chapman-Jouguet reactive wave with a bump.

The second critical point is a turning point in the domain $(\beta > 0, c > c^{cj})$.

Theorem 1.4. (Turning point $(\bar{\beta}, \bar{c})$) *There exists a turning point $(\bar{\beta}, \bar{c})$ which verifies the following properties:*

- (i) $\beta_0(\bar{c}) = \bar{\beta}$, $\beta_0'(\bar{c}) = 0$;
- (ii) $0 < \bar{\beta} \leq \beta_0(c)$ for all $c \geq c^{cj}$;
- (iii) at the turning point $(\bar{\beta}, \bar{c})$, there is a strong reactive wave of special type;
- (iv) for $\beta \in (0, \bar{\beta})$ and $c > c^{cj}$, there is a strong reactive wave with a bump.

A significant consequence is that:

Corollary 1.5. *There is a continuum of admissible speed $\{c \geq c^{cj}\}$ whenever $\beta \in (0, \bar{\beta})$.*

Remark 1.6. *In Figure 1 there is a unique turning point for the function $\beta_0(c)$. But this is only numerical evidence that remains to be proven.*

1.3. Organization of the paper. We focus on the region $\{\xi < 0\}$ and the vector field

$$(1.15) \quad X := \begin{cases} T_\xi = \frac{1}{\beta} \{-cT + \frac{1}{2}T^2 + q_0(1 - Z)\}, \\ Z_\xi = K\varphi(T)Z^\alpha. \end{cases}$$

that we shall consider as a slow-fast system for $\beta \rightarrow 0$. As in [24, 26], we introduce the *fast time*

$$(1.16) \quad \tau = \frac{\xi}{\beta};$$

Denoting by $\dot{}$ the differentiation in τ , the field X turns into

$$(1.17) \quad \tilde{X} := \begin{cases} \dot{T} = -cT + \frac{1}{2}T^2 + q_0(1 - Z), \\ \dot{Z} = \beta K\varphi(T)Z^\alpha. \end{cases}$$

First of all, because we are interested in small viscosity, unlike [24, 26] we perform a straightforward change of variable in (1.17) that maintains β in the system. We simply set:

$$(1.18) \quad \tilde{\beta} = \beta K,$$

and hereafter omit the tilde. Therefore, we will consider the following slow-fast system on $Q = \{(T, Z) \in \mathbb{R}^2 \mid T \geq T_i, Z \geq 0\}$:

$$(1.19) \quad \tilde{X} := \begin{cases} \dot{T} = -cT + \frac{1}{2}T^2 + q_0(1 - Z), \\ \dot{Z} = \beta\varphi(T)Z^\alpha. \end{cases}$$

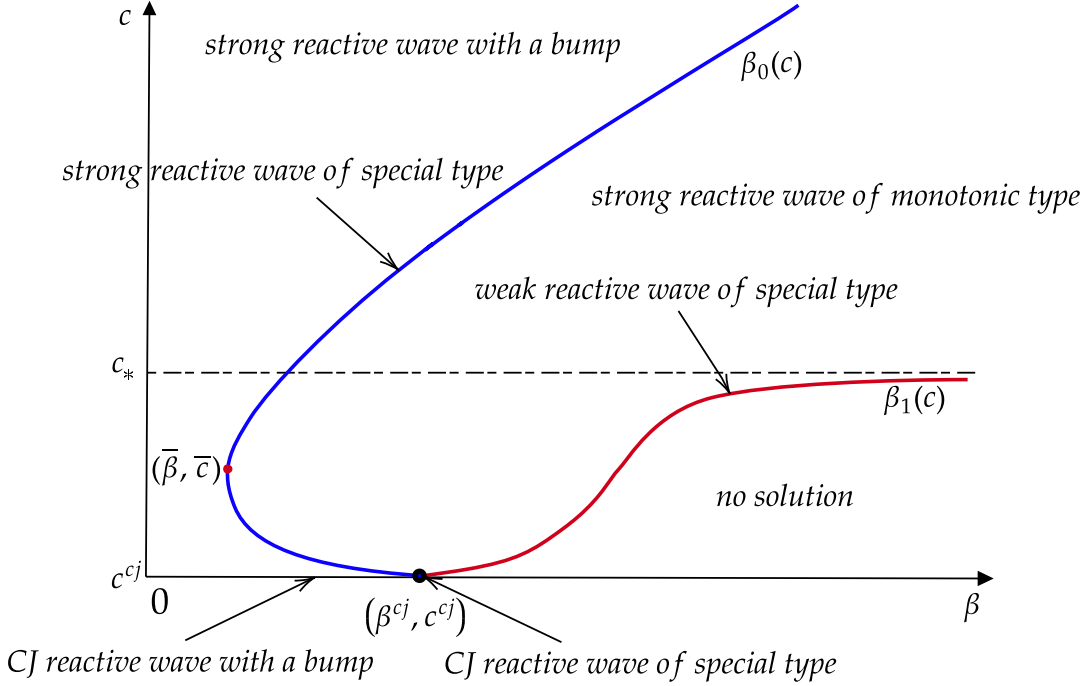


FIGURE 1. This figure provides a qualitative representation of the bifurcation diagram. Note that the only unproven point in this paper concerns the monotonicity of the branch of reactive waves of special type. Thus far, it has only been proven that this branch is locally the graph of β as a function of c .

We write $P_c(T) = -cT + \frac{1}{2}T^2 + q_0$. The roots of P_c are $T_0(c) = c + \sqrt{c^2 - 2q_0}$ and $T_1(c) = c - \sqrt{c^2 - 2q_0}$ (see above), the zeros of \tilde{X} on Q are $(T_0(c), 0)$ and $(T_1(c), 0)$. Also, \tilde{X} has a quadratic contact with the vertical line $\{T = T_i\}$ at the point $(T_i, Z_i(c))$ where $Z_i(c) = \frac{1}{q_0}P_c(T_i)$. The point $(T_i, Z_i(c))$ belongs to Q only if $T_1(c) \geq T_i$ which is the condition $c \leq c_*$, see (1.14).

Section 2 is devoted to the study of the phase portraits. At the outset, we introduce the new variable $U = \frac{1}{1-\alpha}Z^{1-\alpha}$. Making the change of coordinates $\Phi := (T, Z) \rightarrow (T, U)$, the field \tilde{X} becomes $\tilde{X}^U = \Phi_*(\tilde{X})$

$$(1.20) \quad \tilde{X}^U := \begin{cases} \dot{T} = -cT + \frac{1}{2}T^2 + q_0 \left(1 - (1-\alpha)^{\frac{1}{1-\alpha}} U^{\frac{1}{1-\alpha}}\right), \\ \dot{U} = \beta\varphi(T), \end{cases}$$

the big advantage being that the vector field \tilde{X}^U has no zero on Q . There are two particular orbits which are crucial for the study of the problem: the orbit $\gamma_1(\beta, c)$ starting at the point $(T_1(c), 0)$ and arriving at a point $(T_i, U_1(\beta, c))$ and the orbit $\gamma_0(\beta, c)$ starting at the point $(T_0(c), 0)$ and arriving at a point $(T_i, U_0(\beta, c))$. Then, we deduce the phase portrait of \tilde{X} from the one of \tilde{X}^U by taking its image by the map Φ^{-1} . The case of the Chapman Jouguet velocity c^{cj} is the subject of Subsection 2.3.

In Section 3, we study the nature of the trajectory in negative times of \tilde{X} , passing through $(T_i, 1)$ in function of the parameter (β, c) . More specifically, we want to determine if this trajectory is a solution and identify its type. We first consider in Subsection 3.2 the limit cases at fixed $c \geq c^{ej}$, namely $\beta \rightarrow 0$ and $\beta \rightarrow \infty$. Without resorting to the technicalities of the theory of slow-fast systems, we are satisfied with a basic proof: the orbit through the point $(T_i, 1)$ is a solution with a bump. For $\beta = +\infty$, there is a vertical vector field $\tilde{X}_{\infty, c}^U$ without zeros. In Subsection 3.4, we prove a *rotating property* (see [9]) for the vector field $\tilde{X}_{\beta, c}^U$, in function of the parameters β and c .

Section 4 is devoted to the bifurcation diagram in the (β, c) space and to the rigorous proofs of Theorems 1.2, 1.3 and 1.4 which can be inferred from the previous sections. The bifurcation curves $\beta = \beta_1(c)$ and $\beta = \beta_0(c)$ are simple curves for $c > c^{ej}$. In a small neighborhood of the point (β^{ej}, c^{ej}) , the union of the graphs of $\beta_0(c)$ and $\beta_1(c)$ is also a simple curve, to be denoted by (B) .

The behavior as c and β tend to $+\infty$ is trickier and is the subject of Subsection 4.3. As little is known about the behavior of the function $\beta_0(c)$ in the large, we introduce another technical hypothesis (H_∞) about the function φ for large T , which is verified by the two examples: the function $\psi(V) = \varphi(\frac{1}{V})$ is smooth at $V = 0$ with a value $\psi(0) > 0$. We prove that $\beta_0(c) \rightarrow +\infty$ if $c \rightarrow +\infty$, see Proposition 4.4. The lengthy proof is divided in several steps. In particular, we use the Fenichel theory in the specific case of two-dimensional smooth slow-fast systems which shows existence of center manifolds (see [7]), and compute an expansion of a center manifold explicitly.

Finally, to confirm our theoretical results, we performed numerical computations for the bifurcation diagram in Section 5, starting from the vector field:

$$(1.21) \quad \tilde{X}^U := \begin{cases} \dot{T} = -cT + \frac{1}{2}T^2 + q_0 \left(1 - (1 - \alpha)^{\frac{1}{1-\alpha}} U^{\frac{1}{1-\alpha}}\right), \\ \dot{U} = \beta \varphi(T). \end{cases}$$

Two methods are implemented: an analytical method for the Heaviside function in the special case $\alpha = 0.5$ (see Appendix A) and a shooting method for the Arrhenius law (see Appendix B). In particular, our numerical results show an almost complete overlap of the two curves produced by the two methods for the Heaviside function. It is also worth noting a consistent behavior of the bifurcation curves $\beta_0(c)$ and $\beta_1(c)$ across different modeling scenarios (Heaviside and Arrhenius). This similarity suggests that the underlying dynamics of the system is robust to variations in the functional form of the reaction rate. Finally, we note that numerically we have observed a single turning point $(\bar{\beta}, \bar{c})$. In future research, it is expected that the global uniqueness of the turning point will be proved.

2. PHASE PORTRAITS

We consider the vector field

$$(2.1) \quad \tilde{X} := \begin{cases} \dot{T} = -cT + \frac{1}{2}T^2 + q_0(1 - Z), \\ \dot{Z} = \beta \varphi(T)Z^\alpha \end{cases}$$

on $Q = \{(T, Z) \in \mathbb{R}^2 \mid T \geq T_i, Z \geq 0\}$ and write $P_c(T) = -cT + \frac{1}{2}T^2 + q_0$. We introduce the homocline $h_c := \{Z = \frac{1}{q_0}P_c(T)\}$. Along this curve the field is vertical. This line will be used in order to obtain some differentiable properties of the flow of \tilde{X} .

For convenience, we recall $c_* = \frac{T_i^2 + 2q_0}{2T_i}$ (see (1.14)). If $c < c_*$, h_c has two connected components h_c^l and h_c^r which are two arcs of parabola : h_c^l from $(T_1(c), 0)$ to $(T_i, Z_i(c))$ and h_c^r going from $(T_0(c), 0)$ to infinity. If $c > c_*$ we have just one connected component h_c^r .

In order to simplify the arguments about the phase portrait of \tilde{X} , in Section 2.1 we introduce the new variable $U = \frac{1}{1-\alpha}Z^{1-\alpha}$ and make the change of coordinates:

$$\Phi := (T, Z) \rightarrow (T, U).$$

If $c < c_*$, $Q \setminus h_c$ has three connected components: the central region C_c above h_c , the left region L_c below h_c^l and the right region R_c below h_c^r . For $c \geq c_*$, we have just the two regions C_c and R_c . See Figure 2 in (T, U) -coordinates or Figure 3 in (T, Z) -coordinates. The boundary of C_c is equal to $\partial C_c = h_c \cup [T_1(c), T_0(c)] \times \{0\}$.

2.1. Phase portrait of \tilde{X}^U . We introduce the new variable $U = \frac{1}{1-\alpha}Z^{1-\alpha}$ and make the change of coordinates :

$$\Phi := (T, Z) \rightarrow (T, U).$$

In coordinates (T, U) , the field \tilde{X} becomes $\tilde{X}^U = \Phi_*(\tilde{X})$ given by:

$$(2.2) \quad \tilde{X}^U := \begin{cases} \dot{T} = -cT + \frac{1}{2}T^2 + q_0 \left(1 - (1-\alpha)^{\frac{1}{1-\alpha}} U^{\frac{1}{1-\alpha}}\right), \\ \dot{U} = \beta\varphi(T). \end{cases}$$

Note that \tilde{X}^U has no more zero, in fact it has a non-zero vertical component and in particular is transverse to the axis $\{U = 0\}$. Moreover, it is more differentiable than \tilde{X} , which results from the fact that the change of coordinates is itself not differentiable along $\{Z = 0\}$. The non-differentiability is translated into the first line, but \tilde{X}^U is at least of class $[\frac{1}{1-\alpha}] \geq 1$. Then, we can apply the Cauchy theorem to \tilde{X}^U on the whole closed domain Q . This implies the *uniqueness of trajectories* through each point of Q . We shall show that this is not the case for \tilde{X} .

The vertical lines are preserved by the mapping $\Phi := (T, Z) \mapsto (T, U)$ which is a smooth diffeomorphism on $Q^+ = \{T \geq T_i, Z > 0\}$. All the differentiable properties verified on Q^+ are preserved, for instance X^U has also a quadratic contact with $\{T = T_i\}$ at $(T_i, U_i(c))$ where $(1-\alpha)^{\frac{1}{1-\alpha}} U_i(c)^{\frac{1}{1-\alpha}} = \frac{1}{q_0} P_c(T_i)$. Also the homocline of \tilde{X} is sent on the homocline of \tilde{X}^U . We keep the same names as before for the homocline, its connected components and the connected components of $Q \setminus h_c$. The homocline h_c is now given by $\{(1-\alpha)^{\frac{1}{1-\alpha}} U^{\frac{1}{1-\alpha}} = \frac{1}{q_0} P_c(T)\}$. At the points $(T_0(c), 0)$ and $(T_1(c), 0)$ this homocline has a contact of order $\frac{1}{1-\alpha}$ with the vertical, which is the direction of \tilde{X}^U at these points. Elsewhere, h_c remains transverse to the vertical direction.

As the vector field \tilde{X}^U has no zero on Q , it is easy to describe its phase portrait on this domain, using the qualitative ideas of Poincaré (see [1, 21]; more recent references include [8, 16, 22]). Nevertheless, minor difficulties arise from the non-compactness of Q . We proceed by giving a series of claims:

Claim 2.1. *Each orbit γ (curve image of trajectory) is a graph $U \mapsto \tilde{T}_\gamma(U)$ above some interval in U .*

Claim 2.2. *Each orbit γ has at most one intersection point (T_γ, U_γ) with ∂C_c . When $U_\gamma > 0$, i.e. when $(T_\gamma, U_\gamma) \notin [T_1(c), T_0(c)] \times \{0\}$, the function $\tilde{T}_\gamma(U)$ has a maximum at U_γ .*

Proof. The first claim comes from the fact that \tilde{X}^u has a non-zero vertical direction and then each orbit γ is a graph $U \mapsto \tilde{T}_\gamma(U)$ above some interval in U . Next, as \tilde{X}^u points upward along ∂C_c each orbit γ cuts ∂C_c in at most one point. At a point (T_γ, U_γ) of γ where \tilde{X}^U is vertical, the function \tilde{T}_γ has a zero-derivative at U_γ . Along γ , the vector field \tilde{X}^U has a positive slope if $U < U_\gamma$ and a negative slope if $U > U_\gamma$: the function \tilde{T}_γ has a maximum at U_γ . \square

Claim 2.3. *Let be $U_0 > U_i(c)$. The trajectory through the point (T_i, U_0) arrives in a finite negative time on $\partial C_c = h_c \cup [T_1(c), T_0(c)] \times \{0\}$.*

Proof. We look at the trajectory $\varphi(\tau)$ of \tilde{X}^U through the point (T_i, U_0) , in negative times. This trajectory remains in the strip $S = \{0 \leq U \leq U_0\}$. As $B = S \cap C_c$ is compact, it follows from the Poincaré-Bendixson theorem (see, e.g., [1, 21]) that $\varphi(\tau)$ arrives in a finite negative time τ_0 at a point m_0 in boundary ∂B of B . This time τ_0 is strictly negative because $U_0 > U_i(c)$ and then the U -coordinate of m_0 is strictly smaller than U_0 (the coordinate U is strictly decreasing along the trajectory). Then m_0 belongs to the part of ∂B contained in ∂C_c . \square

Claim 2.4. *Conversely, the trajectory of X^U by any point of ∂C_c is contained in C_c : it goes upward and toward the left and arrives on $\{T_i\} \times [U_i(c), +\infty)$ in a finite positive time.*

Proof. Take any point $m \in \partial C_c$. As any trajectory must enter into C_r in positive times (for $m = T_1(c)$ or $T_0(c)$, it is convenient to use a tubular neighborhood), and cuts at most one time ∂C_c by Claim 2.1, the (positive) trajectory of m is entirely contained in C_c . It is clear that a positive trajectory in C_c goes upward and toward the left.

It remains to prove that this trajectory arrives on $\{T_i\} \times [U_i(c), +\infty)$ in a finite positive time. We proceed in two steps. First we choose an $\bar{U} > U_i(c)$ also greater than the U -coordinate of m . We call now M the compact part of C_c below the horizontal line $\{U = \bar{U}\}$. Using the Poincaré-Bendixson theorem we have that the trajectory through m arrives in a finite positive time at a point in $\{T_i\} \times [U_i(c), \bar{U}]$ or in $\{U = \bar{U}\}$. In the first case we have finished. In the second case, we arrive at a point $p' = (\bar{T}, \bar{U}) \in C_c$, with $\bar{T} > T_i$.

We proceed to the second step of the proof, considering the trajectory from p' , in the positive time. This trajectory remains in the vertical strip $S = \{U \geq \bar{U}, T \leq \bar{T}\}$ and it is clear that there exists a $A > 0$ such that the horizontal component of \tilde{X}^U is less than $-A$ on S (on the segment $\{(T, \bar{U}) | T \in [T_i, \bar{T}]\}$, this horizontal component is strictly negative and then less than $-A$ for some $A > 0$, by compactness; moreover this component is decreasing when U increases). On the other side, the vertical component of \tilde{X}^U is positive and less than βB , where $B = \text{Max}\{\varphi(T) | T \in [T_i, \bar{T}]\} > 0$. From these two estimations it follows trivially that the trajectory through p' arrives on $\{T = T_i\}$ in a finite positive time. \square

Claim 2.5. *Any trajectory starting at a point of $h_r \setminus \{(T_0(c), 0)\}$ arrives in a finite negative time at a point $(T, 0)$ with $T > T_0(c)$.*

Proof. As such a trajectory remains in a compact subset of R_c , we can again apply the Poincaré-Bendixson theorem to prove it arrives in a finite negative $-\tau_0 < 0$ at a point $(T, 0)$ with $T \geq T_0(c)$. Of course we have that $T > T_0(c)$ because if $T = T_0(c)$ the trajectory would be, as consequence of (4), in the interior of C_c for any time $-\tau$, with $-\tau_0 < -\tau < 0$, that is impossible. \square

It is now very easy to draw the phase portrait of \tilde{X}^U , see Figure 2. It is important to notice that the vector field is transverse to the horizontal axis $\{U = 0\}$, tilted to the left along the interval $]T_1(c), T_0(c)[$ (i.e. has a negative slope) and tilted to the right outside (i.e. has a positive

slope). There are two particular orbits : the orbit $\gamma_1(\beta, c)$ starting at the point $(T_1(c), 0)$ and arriving at a point $(T_i, U_1(\beta, c))$ and the orbit $\gamma_0(\beta, c)$ starting at the point $(T_0(c), 0)$ and arriving at a point $(T_i, U_0(\beta, c))$. These orbits are crucial for proving the results of Section 3. At $(T_0(c), 0)$ and $(T_1(c), 0)$ these orbits have a vertical tangent, but it is possible to prove more by a direct computation:

Lemma 2.6. *Let be $i = 0$ or 1 . There are constants $k_i > 0$, depending on the parameter (β, c) , such that : putting $T = T_i(c) + x$, the orbit $\gamma_i(\beta, c)$ has the asymptotic $x \sim -k_i U^{\frac{2-\alpha}{1-\alpha}}$.*

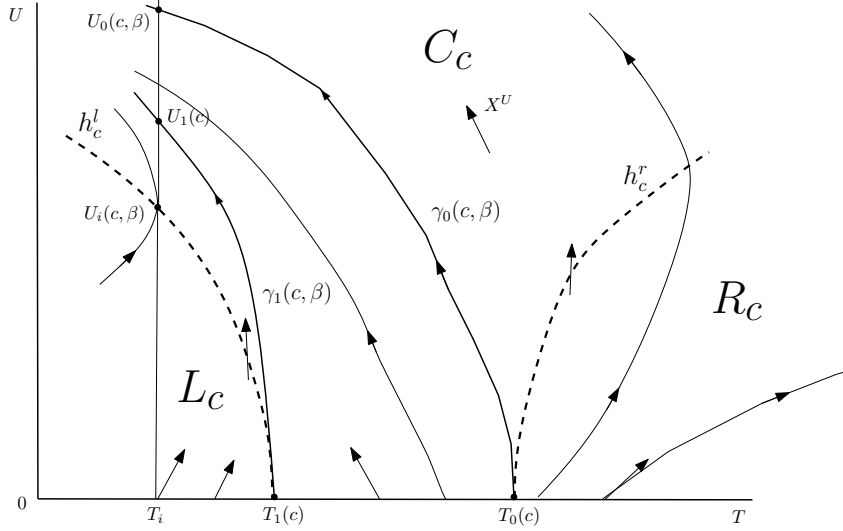


FIGURE 2. Phase portrait of \tilde{X}^U for $c > c^{ej}$

2.2. Phase portrait of \tilde{X} . We now infer the phase portrait of \tilde{X} from the one of \tilde{X}^U , by taking its image by the map Φ^{-1} .

Outside $\{Z = 0\}$, image of $\{U = 0\}$, the phase portraits are the same, up the diffeomorphism $\Phi^{-1}|_{Q^+}$ (which also preserves the time). The only differences occur along the axis $\{Z = 0\}$. To obtain the asymptotics of the orbits along this axis we will use the following elementary results:

Lemma 2.7. (i) *If a curve γ has, at a point $(T_*, 0)$, an asymptotic $T - T_* \sim kU^\delta$ with $k \in \mathbb{R} - \{0\}$ and $\delta > 0$, then its image $\Phi^{-1}(\gamma)$ has an asymptotic $T - T_* \sim \frac{k}{1-\alpha} U^{\delta(1-\alpha)}$.*

(ii) *As a consequence, for $\delta(1-\alpha) < 1$ (for instance, for $\delta = 1$), $\Phi^{-1}(\gamma)$ is tangent to $\{Z = 0\}$ with order $\frac{1}{\delta(1-\alpha)}$ on a side determined by the sign of k ; for $\delta(1-\alpha) > 1$, $\Phi^{-1}(\gamma)$ is tangent to the vertical with order $\delta(1-\alpha)$, on a side determined by the sign of k .*

The axis $\{Z = 0\}$ is invariant: it contains two singular points $(T_1(c), 0)$, $(T_0(c), 0)$ and three regular orbits. The most remarkable fact, following from Lemma 2.7, is that other orbits arrive tangentially on the axis $\{Z = 0\}$ in negative time, with a contact of order $\frac{1}{1-\alpha}$, save the two orbits “arriving” to the singular points $(T_1(c), 0)$ and $(T_0(c), 0)$. The contact is on the left for an orbit arriving at $(\bar{T}, 0)$ for $T_1(c) < \bar{T} < T_0(c)$ and on the right for $\bar{T} < T_1(c)$ or $\bar{T} > T_0(c)$. At $(T_1(c), 0)$ and $(T_0(c), 0)$ the orbits arrive transversality to $\{Z = 0\}$, tangent to the vertical

direction and on the left. We write these orbits : $\gamma_1(\beta, c)$ and $\gamma_0(\beta, c)$, respectively. This follows from Lemmas 2.6 and 2.7 implying that the asymptotics is $T - T_j(c) \sim -\bar{k}_j Z^{(2-\alpha)}$, for a $\bar{k}_j > 0$, for $j = 0$ or 1 . These trajectories cut transversely the verticals $\{T = T_i\}$ at the points $(T_i, Z_1(\beta, c))$ and $(T_i, Z_0(\beta, c))$, respectively.

A consequence is that *the vector field \tilde{X} does not satisfy the Cauchy property of uniqueness of trajectory*: at any point $(T, 0)$, with $T \neq T_1(c), T_0(c)$ arrive two trajectories : one is horizontal and the other is the image by Φ^{-1} of the trajectory of X^U . Inversely, it is easy to see that, starting at any point (T_i, Z) , with $Z > Z_1(\beta, c)$, and going in negative time, we arrive at a point $(\bar{T}, 0)$ in the finite (fast) time τ_Z (equal to $\frac{Z^{1-\alpha}}{(1-\alpha)\beta}$ in the Heaviside case) and next, if $Z \neq Z_0(\beta, c)$, we slide an infinite time along $\{Z = 0\}$, towards the point $(T_0(c), 0)$.

The phase portrait is given in Figure 3. The point $(T_0(c), 0)$ is a degenerate repulsive node

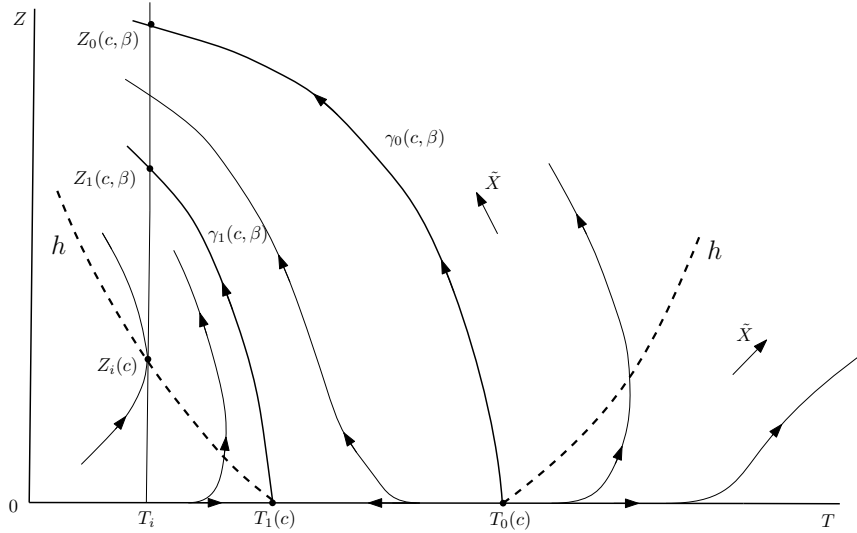


FIGURE 3. Phase portrait of \tilde{X} for $c > c^{ej}$

and the point $(T_1(c), 0)$ is a degenerate saddle of \tilde{X} . The basin (of repulsion) of $(T_0(c), 0)$ is at the right of the orbit $\gamma_1(\beta, c)$. For each $Z > Z_1(c)$ the trajectory through (T_i, Z) tends toward $(T_0(c), 0)$ for negative times. This time is finite if $Z = Z_0(\beta, c)$ and infinite otherwise. For $Z_1(\beta, c) < Z < Z_0(\beta, c)$ the trajectory arrives by the left side and is a monotonic graph $T(Z)$. For $Z > Z_0(\beta, c)$, the trajectory arrives by the rightarrow side after a unique bump (it has to cut the homoclinic branch h_c^r only one time). The orbit $\gamma_0(\beta, c)$, that we say of *finite time* type, separates the two types that we will call here *monotonic and bump orbit*, respectively, see Section 1.2.

Claim 2.8. *There is a solution if and only it holds:*

$$(2.3) \quad T_1(c) \leq T_i \quad \text{or} \quad Z_1(\beta, c) < 1.$$

This solution is of monotonic, finite time or bump type (see Section 1.2), respectively, depending on the position of 1 : $Z_1(\beta, c) < 1 < Z_0(\beta, c)$, $Z_0(\beta, c) < 1$ or $1 = Z_0(\beta, c)$, respectively.

We intend to address these issues in the next section by looking at the position of $Z_1(\beta, c)$ and $Z_0(\beta, c)$ against the value 1, in function of the parameter (β, c) .

2.3. The Chapman-Jouguet case. In the previous subsections and in particular in Figures 2 and 3, we have implicitly assumed that $c > c^{cj} = \sqrt{2q_0}$. The limit case $c = c^{cj}$ can be treated in the same way. In this case, we have that $T_1(c^{cj}) = T_0(c^{cj}) = \sqrt{2q_0}$.

As above, we begin with the phase portrait of \tilde{X}^U . The two branches $h_{c^{cj}}^l$ and $h_{c^{cj}}^r$ start from the point $(0, c^{cj})$ with a contact of order $\frac{1}{1-\alpha}$. The two orbits $\gamma_i(\beta, c^{cj})$ coincide now in a single orbit $\gamma(\beta, c^{cj})$ which is contained in the region $C_{c^{cj}}$. This follows from Lemma 2.7, but it is also clear for topological reasons. Then, we have that $U_0(\beta, c^{cj}) = U_1(\beta, c^{cj})$. From the phase portrait of \tilde{X}^U we can deduce the one of \tilde{X} as above. A possible solution, which exists if and only if $1 > Z_0(c^{cj})$, is always of bump type. The phase portraits of \tilde{X}^U and \tilde{X} are presented in Figure 4. The vector field \tilde{X} has a unique singular point $(c^{cj}, 0)$. This point is a degenerate

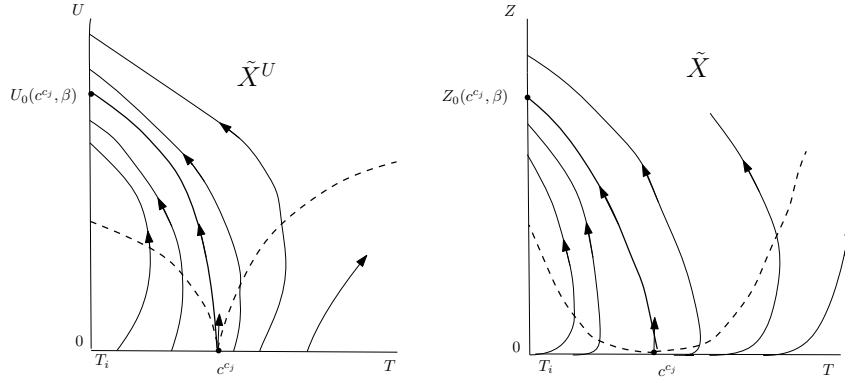


FIGURE 4. Phase portraits for $c = c^{cj}$

saddle-node singularity. The orbit $\gamma(\beta, c^{cj})$ is an unstable separatrix which separates the saddle type sector from the node type sector. When c increases, this point bifurcates into the pair of a degenerate saddle and a degenerate node appearing in Figure 3.

3. EXISTENCE OF A SOLUTION IN FUNCTION OF (β, c)

We have in mind to study the nature of the trajectory in negative times of \tilde{X} , passing through $(T_i, 1)$ in function of the parameter (β, c) . Our goal is to determine if this trajectory is a solution and identify its type. To emphasize that \tilde{X} depends on the parameter (β, c) , we will write it as $\tilde{X}_{\beta, c}$ in this section and the next one.

3.1. Property for c large. First, we fix any value of $\beta > 0$ and look at how it depends on c . It is given by the elementary result:

Lemma 3.1. *If $c \geq c_\star = \frac{T_i^2 + 2q_0}{T_i}$, we have that $T_1(c) \leq T_i$ and therefore the degenerate saddle point $(T_1(c), 0)$ no longer belongs to $(T_i, +\infty)$. We are in the first case of the claim 2.8: $(T_i, 1)$ belongs to the basin of $(T_0(c), 0)$ and the trajectory of this point, for negative times, is a solution (of one type or the other).*

3.2. Properties for β near 0 and $+\infty$. We now fix any value of $c \geq c^{cj}$ and we look at the variation of β from 0 to $+\infty$.

3.2.1. Slow analysis for $\beta \rightarrow 0_+$. We have a *slow-fast system* in dimension 2, with small parameter β , see [7] for detailed definitions and properties. As the parameter c is fixed, we will usually skip it.

For convenience, we consider the system $-\tilde{X}_{\beta,c}$. The *limit equation* $-\tilde{X}_{c,0}$ for $\beta = 0$ has a very simple phase portrait: h_c is a curve of zeros (called the *critical curve*). The dynamics outside this critical curve (namely the fast dynamics) is horizontal, without singularities. Here, we just need to consider the vector field $-\tilde{X}_{\beta,c}$ on $Q^+ = Q \cap \{Z > 0\}$. On Q^+ , the vector field $-\tilde{X}_{\beta,c}$ is smooth. The two branches of h_c are normally hyperbolic arcs of zeros, h_c^r is attracting and h_c^l repulsive. For any $\beta > 0$, small, we are interested in the orbit of Γ_β of $-\tilde{X}_{\beta,c}$ starting at the point $(T_i, 1)$. We want to prove that, for $\beta > 0$ small enough, we will have $1 > Z_0(\beta, c)$,

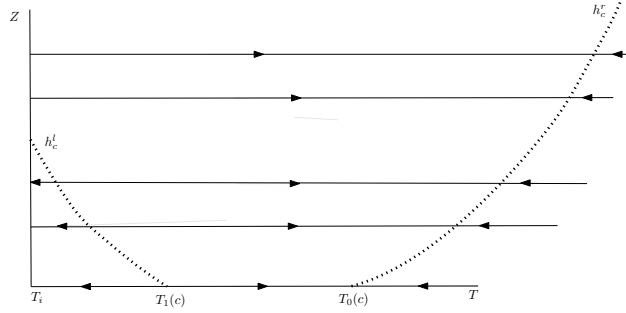


FIGURE 5. The limit vector field for $\beta = 0$

that is, we have a bump solution.

We will give a very basic proof here, which will not use the technicalities of the theory of slow-fast systems as in [7].

Let $\{T = h(Z)\}$ the equation of the branch h_c^r . The function $h(Z)$ is smooth and $h'(Z) > 0$ for $Z > 0$. We choose any interval $[Z_b, Z_a]$ such that $0 < Z_b < 1 < Z_a$. and associate with any $\delta > 0$ a tubular neighborhood

$$\mathcal{T}_\delta = \{Z_a \leq Z \leq Z_b, h(Z) - \delta \leq T \leq h(Z) + \delta\}.$$

\mathcal{T}_δ is a thin curved rectangle with corners

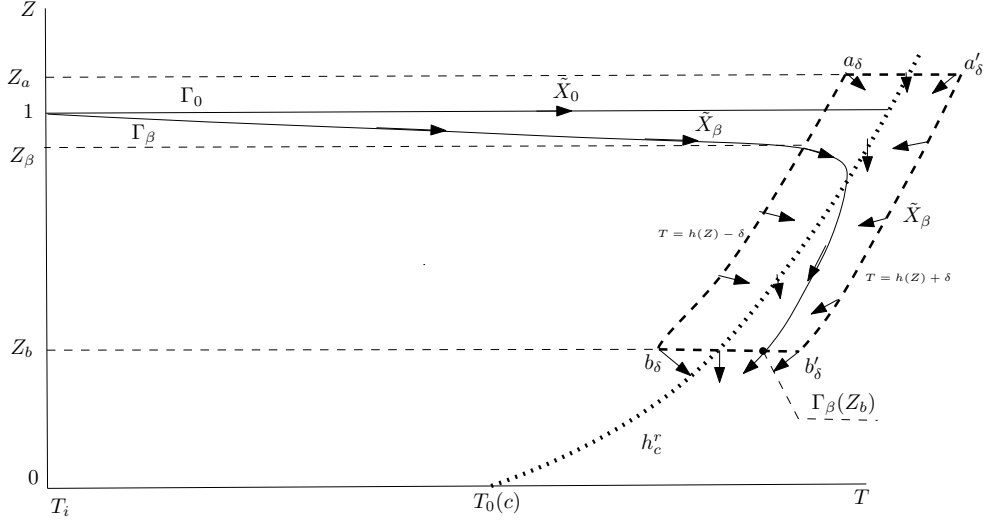
$$\begin{aligned} a_\delta &= (h(Z_a) - \delta, Z_a), & a'_\delta &= (h(Z_a) + \delta, Z_a) \\ b_\delta &= (h(Z_b) - \delta, Z_b), & b'_\delta &= (h(Z_b) + \delta, Z_a). \end{aligned}$$

We will note $[a_\delta, a'_\delta]$, $[b_\delta, b'_\delta]$, $[a_\delta, b_\delta]$ and $[a'_\delta, b'_\delta]$ the four sides of \mathcal{T}_δ (see Figure 6). If $\delta > 0$ is small enough, the following condition (R) is fulfilled:

$$(R) \quad h(1) - \delta > h(Z_b) + \delta.$$

Recall that any orbit of $-\tilde{X}_{\beta,c}$ through a point (T_i, \bar{Z}) and for any $\beta > 0$ is a graph above an interval of the vertical Z -axis. The following proposition proves that, for $\beta > 0$ small enough, the orbit Γ_β through the point $(T_i, 1)$ is a solution of bump type. As follows from the analysis presented in Section 1, it is sufficient to prove that Γ_β cuts the homocline branch h_c^r .

Proposition 3.2. *Choose any $\delta > 0$, verifying the condition (R). We consider the orbit Γ_β of $-\tilde{X}_{\beta,c}$, starting at the point $(T_i, 1)$. If $\beta > 0$ is small enough, Γ_β is defined at least above the*

FIGURE 6. Trapping the solution for β small.

interval $[Z_b, 1]$ as a graph of a smooth function $T = \varphi_\beta(Z)$. There is a $\bar{Z}_\beta \in (Z_b, 1)$ such that $\varphi'_\beta(\bar{Z}_\beta) = 0$. As a consequence, Γ_β cuts the homocline branch h_c^r and then is a solution of bump type. This implies that $Z_0(\beta, c) < 1$ if $\beta > 0$ is small enough.

Proof. Choose a $\delta > 0$ verifying the condition (R) and consider the orbit Γ_β through $(T_i, 1)$. It is the graph of a function $T = \varphi_\beta(Z)$, smooth for $Z > 0$. If $\beta > 0$ is small enough, Γ_β contains an arc between $(T_i, 1)$ and a point $(h(Z_\beta) - \delta, Z_\beta)$, located at the boundary of \mathcal{T}_δ below the point a_δ . Moreover $Z_\beta \rightarrow 1_-$ for $\beta \rightarrow 0$ and the arc of Γ_β above $[Z_\beta, 1]$ converges smoothly toward the horizontal. This means in particular that φ_β is defined in a neighborhood of 1, with $\varphi_\beta(Z_\beta) = h(Z_\beta) - \delta$, and that $\varphi'_\beta(1) \rightarrow -\infty$ when $\beta \rightarrow 0$.

We look now at the continuation of Γ_β from the point $(h(Z_\beta) - \delta, Z_\beta)$. First, we observe that the rectangle \mathcal{T}_δ has a *trapping property*: for any $\beta > 0$, the vector field $-\tilde{X}_\beta$ is transversely pointing inward along the three sides $[a_\delta, a'_\delta]$, $[a'_\delta, b'_\delta]$, $[a_\delta, b_\delta]$ and transversely pointing outward along the last side $[b_\delta, b'_\delta]$. Moreover, $-\tilde{X}_\beta$ has no singular point inside \mathcal{T}_δ . Then, it follows from the Poincaré-Bendixson theorem that the trajectory entering the rectangle at the point $(h(Z_\beta) - \delta, Z_\beta) \in [a_\delta, b_\delta]$ must reach a point in $[b_\delta, b'_\delta]$. This means that φ_β is defined on $[Z_b, 1]$ and that $\varphi_\beta(Z_b) \in [h(Z_a) - \delta, h(Z_b) + \delta]$, and in particular it holds

$$(3.1) \quad \varphi_\beta(Z_b) < h(Z_b) + \delta.$$

Now, as $Z_\beta \rightarrow 1$ for $\beta \rightarrow 0$, it follows from condition (R) that

$$(3.2) \quad h(Z_\beta) - \delta > h(Z_b) + \delta,$$

if $\beta > 0$ is small enough.

By definition, $h(Z_\beta) - \delta = \varphi_\beta(Z_\beta)$. Then it follows from (3.1) and (3.2) that $\varphi_\beta(Z_b) < \varphi_\beta(Z_\beta)$. As $Z_\beta > Z_b$, the mean value theorem implies that there exists a $\bar{Z}_1 \in]Z_b, Z_\beta[$ such that $\varphi'_\beta(\bar{Z}_1) > 0$. As $\varphi'_\beta(1) < 0$ for $\beta > 0$ small enough, it eventually follows from the intermediary

value theorem that there exists a $\bar{Z}_\beta \in (\bar{Z}_1, 1) \subset (Z_b, 1)$ such that $\varphi'_\beta(\bar{Z}_\beta) = 0$. This completes the proof. \square

Remark 3.3. *Using the general theory of slow-fast systems, it is possible to obtain additional properties of the flow when $\beta \rightarrow 0$. For example, one can prove that $Z_0(\beta, c)$ and $Z_1(\beta, c)$ tends toward $Z_i(c)$ when $\beta \rightarrow 0$.*

3.2.2. Limit for $\beta \rightarrow +\infty$. To look at the limit $\beta \rightarrow +\infty$, it is better to return to the initial vector field which we now write $X_{\beta,c}$, and to the slow time ξ . We also introduce the corresponding vector field

$$(3.3) \quad X_{\beta,c}^U := \begin{cases} \dot{T} = \frac{1}{\beta} \left[-cT + \frac{1}{2}T^2 + q_0 \left(1 - (1-\alpha)^{\frac{1}{1-\alpha}} U^{\frac{1}{1-\alpha}} \right) \right], \\ \dot{U} = \varphi(T). \end{cases}$$

For $\beta = +\infty$, we have a vertical vector field, without zeros: $X_\infty^U = \varphi(T) \frac{\partial}{\partial U}$. From this, we can deduce the following result:

Proposition 3.4. *Take any fixed $c \geq c^{ej}$. If $\beta \rightarrow +\infty$, we have that :*

$$Z_1(\beta, c) \rightarrow +\infty \quad \text{and} \quad Z_0(\beta, c) \rightarrow +\infty$$

Proof. Fix a value $c \geq c^{ej}$. Clearly, the vector field $X_{\beta,c}^U$ converges uniformly toward the vertical vector field $\varphi(T) \frac{\partial}{\partial U}$ on each compact subset of Q . This obviously implies that $Z_1(\beta, c)$ and $Z_0(\beta, c)$ take arbitrarily large values when $\beta \rightarrow +\infty$. But since these two functions are strictly increasing, as proved in Proposition 3.9 below, they have to converge toward $+\infty$. \square

3.3. The transition map $Z(T, \beta, c)$. The vector field $\tilde{X}_{\beta,c}^U$ is transverse to the horizontal axis $\{U = 0\}$. From the claim 2.4 of Subsection 2.1, it follows that each trajectory starting at a point of $[T_i, T_0(c)] \times \{0\}$ cuts transversally the vertical axis $\{T = T_i\}$ after a finite time. By continuity, this implies that there exists a $T(\beta, c) > T_0(c)$ such that each trajectory starting at a point of $[T_i, T(\beta, c)] \times \{0\}$ cuts also transversally the vertical axis $\{T = T_i\}$ after a finite time.

This defines a transition map from $[T_i, T(\beta, c)] \times \{0\}$ to $\{T = T_i\}$. Choosing for convenience the variable Z to parametrize the vertical axis, this transition map is a function $Z(T, \beta, c)$ of class $\left[\frac{1}{1-\alpha}\right]$ on the domain:

$$\mathcal{Z} = \{(T, \beta, c) \mid c \in [c^{ej}, +\infty), \beta \in (0, +\infty), T \in [T_i, T(\beta, c)]\}.$$

This follows from the Cauchy theorem and the implicit function theorem.

For each fixed (β, c) , the transition map $T \mapsto Z(T, \beta, c)$ is a diffeomorphism of class $\left[\frac{1}{1-\alpha}\right]$, preserving the orientation. This means that, for all $(T, \beta, c) \in \mathcal{Z}$,

$$(3.4) \quad \frac{\partial Z}{\partial T}(T, \beta, c) > 0.$$

The more interesting values of $Z(T, \beta, c)$ are $Z_1(\beta, c) = Z(T_1(c), \beta, c)$ and $Z_0(\beta, c) = Z(T_0(c), \beta, c)$. Since $Z(T, \beta, c)$ is of class $\left[\frac{1}{1-\alpha}\right]$, we also have that $Z_1(\beta, c)$ and $Z_0(\beta, c)$ are of class $\left[\frac{1}{1-\alpha}\right]$.

3.4. Rotating property. We want to prove a *rotating property* for the vector field $\tilde{X}_{\beta,c}^U$ (see [9]), in function of the parameters β and c . The general definition of the rotating property is as follows:

Definition 3.5. Let X_ε a 1-family of vector fields with parameter $\varepsilon \in (-\varepsilon_0, \varepsilon_0)$, for some small $\varepsilon_0 > 0$, defined on an open connected subset $W \subset \mathbb{R}^2$. We assume that this family is at least C^1 , i.e., that the components are C^1 as functions of $(m, \varepsilon) \in W \times (-\varepsilon_0, \varepsilon_0)$. We say that X_ε has rotating property in function of ε if for all $m \in W$ and all ε , the vectors $X_\varepsilon(m)$ and $\frac{\partial X_\varepsilon}{\partial \varepsilon}(m)$ are linearly independent. Then, $\text{Det}(X_\varepsilon(m), \frac{\partial X_\varepsilon}{\partial \varepsilon}(m))$ has a constant sign on W .

An elementary basic result is the following:

Lemma 3.6. Let W be an open connected subset of \mathbb{R}^2 and X_ε an ε -family of vector field s , of class C^k , for some $k \geq 1$, defined on a neighborhood Q of \overline{W} (the closure of W). We assume that X_ε is on W a rotating family as in Definition 3.5. Let be $p \in \overline{W}$ and $\gamma_\varepsilon(p)$ the positive orbit of X_ε in Q , through p . We assume that γ_0 is contained in \overline{W} , but is not entirely included in $\partial W = \overline{W} \setminus W$.

Let be $q \in \gamma_0(p)$ with $q \neq p$. We choose a transverse section Σ to X_0 through q , with a smooth coordinate s , such that $q = \{s = 0\}$.

Assume that ε_0 is small enough, such that Σ is also transverse to X_ε for all ε and such that $\gamma_\varepsilon(p)$ cuts Σ at a point of coordinate $s = P(\varepsilon)$, for all ε (by assumption $P(0) = 0$). Then, the function $s = P(\varepsilon)$ is C^k and $P'(0) \neq 0$: we have that $P'(0) > 0$ if the vector $\frac{\partial X_\varepsilon}{\partial \varepsilon}(q)$ is oriented in the s -direction and $P'(0) < 0$ if not. See Figure 7.

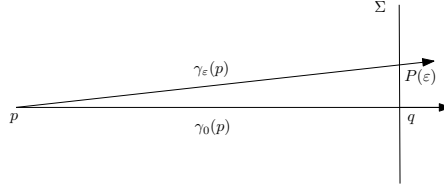


FIGURE 7. The function $P(\varepsilon)$

Proof. Let us remark that the result does not change if we replace X_ε by a family C^k -conjugated (i.e. changed by a C^k -family of diffeomorphisms) or C^k -equivalent (i.e. multiplied by a C^k -family of positive functions). We will use this possibility several times. We will keep the name X_ε for the resulting vector field family.

First, we use the flot box theorem (see, e.g., [8]) in a neighborhood \mathcal{T} of $\gamma_0(p)$ in Q , with local C^k coordinates (x, y) in which, up a C^k -equivalence, we have that $X_0 = \frac{\partial}{\partial x}$, $p = (0, 0)$ and $\Sigma = \{1\} \times [-1, 1]$. In \mathcal{T} , the family takes the form (for $\varepsilon_0 > 0$ small enough and up to C^k families of diffeomorphisms and equivalences):

$$X_\varepsilon := \left(1 + \varepsilon A(x, y, \varepsilon)\right) \frac{\partial}{\partial x} + \varepsilon B(x, y, \varepsilon) \frac{\partial}{\partial y}.$$

As $\gamma_0 \subset \overline{W}$ and changing y if necessary by $-y$, we have that $B(x, 0, 0) \geq 0$ (this means that $\frac{\partial X_\varepsilon}{\partial \varepsilon}$ is oriented in the y -direction along the x -axis). Moreover, the hypothesis that γ_0 is not completely contained in ∂W implies that $B(x, 0, 0) \not\equiv 0$ and then that:

$$(3.5) \quad \int_0^1 B(x, 0, 0) dx > 0.$$

If $\varepsilon_0 > 0$ is small enough we have that $1 + \varepsilon A(x, y, \varepsilon) > 0$, and then, up to C^k -equivalence, we have that:

$$(3.6) \quad X_\varepsilon := \frac{\partial}{\partial x} + \varepsilon \bar{B}(x, y, \varepsilon) \frac{\partial}{\partial y},$$

for a new C^k function $\bar{B}(x, y, \varepsilon) = B(x, y, 0) + O(\varepsilon)$. The equation of trajectories takes the form:

$$(3.7) \quad \tilde{X} := \begin{cases} \dot{x} = 1 \\ \dot{y} = \varepsilon \bar{B}(x, y, \varepsilon). \end{cases}$$

We look at the trajectory of p . For it, we have that $x \equiv t$ and then we can reduce the equation to a single line for a function $y_\varepsilon(x)$ whose $\gamma_\varepsilon(p)$ is the graph:

$$(3.8) \quad \frac{dy_\varepsilon}{dx}(x) = \varepsilon \bar{B}(x, y_\varepsilon, \varepsilon).$$

As $y_\varepsilon(0) = 0$ it follows from (3.8) that $y_\varepsilon(x) = O(\varepsilon)$. Reporting this in (3.8), we have that

$$(3.9) \quad \frac{dy_\varepsilon}{dx}(x) = \varepsilon B(x, 0, 0) + O(\varepsilon^2),$$

where the remainder $O(\varepsilon^2)$ is now a function of (x, ε) , of class C^k . This equation (3.9) implies that

$$(3.10) \quad y_\varepsilon(x) = \varepsilon \int_0^x B(\tau, 0, 0) d\tau + O(\varepsilon^2).$$

As $P(\varepsilon) = y_\varepsilon(1)$, we obtain that $P(\varepsilon)$ is C^k and, using (3.5), that:

$$P'(0) = \int_0^1 B(\tau, 0, 0) d\tau > 0.$$

Clearly, the sign of $P'(0)$ changes if we change the orientation of Σ (i.e. of the y -axis). This finishes the proof. \square

Remark 3.7. *Lemma 3.6 can be proved using the general theory of first order variational equations (see [5]). This theory would give an intrinsic expression for the derivative $P'(0)$.*

We now return to the family $\tilde{X}_{\beta,c}^U$. The vector field $\frac{\partial \tilde{X}_{\beta,c}^U}{\partial \beta}(m) = \varphi(T) \frac{\partial}{\partial U}$ is transverse to $\tilde{X}_{\beta,c}^U$ on C_c . Moreover, the pair $(\tilde{X}_{\beta,c}^U(m), \frac{\partial \tilde{X}_{\beta,c}^U}{\partial \beta}(m))$ has a clockwise orientation. Then, the family $\tilde{X}_{\beta,c}^U$ has the rotating property in the clockwise direction on the open connected set C_c , in function of the parameter $\varepsilon = \beta - \beta_0$ for any $\beta_0 \in (0, +\infty)$. This clockwise orientation implies that $\frac{\partial \tilde{X}_{\beta,c}^U}{\partial \beta}(m)$ is oriented as the Z -axis in comparison to the orbit of $\tilde{X}_{\beta,c}^U$, at any point m of C_c .

We consider the trajectory $\gamma_{\beta_0,c}(T)$ of $\tilde{X}_{\beta_0,c}^U$ starting at any point $(T, 0)$, for $T \in [T_1(c), T_0(c)]$. This trajectory is contained in the closure \bar{C}_c and cuts the boundary ∂C_c only at the starting point $(T, 0)$. Thus, a direct consequence of Lemma 3.6 is the following:

Corollary 3.8. *For $T \in [T_1(c), T_0(c)]$ and any (β, c) , it holds $\frac{\partial Z}{\partial \beta}(T, \beta, c) > 0$.*

Applying this to $T = T_1(c)$ and $T = T_0(c)$, we have the following result:

Proposition 3.9. For $i = 0, 1$ and any fixed value of $c \in [c^{ej}, +\infty)$, the two functions $\beta \mapsto Z_i(\beta, c)$ are of class $[\frac{1}{1-\alpha}]$ in (β, c) . Moreover we have that

$$\frac{\partial Z_i}{\partial \beta}(\beta, c) > 0$$

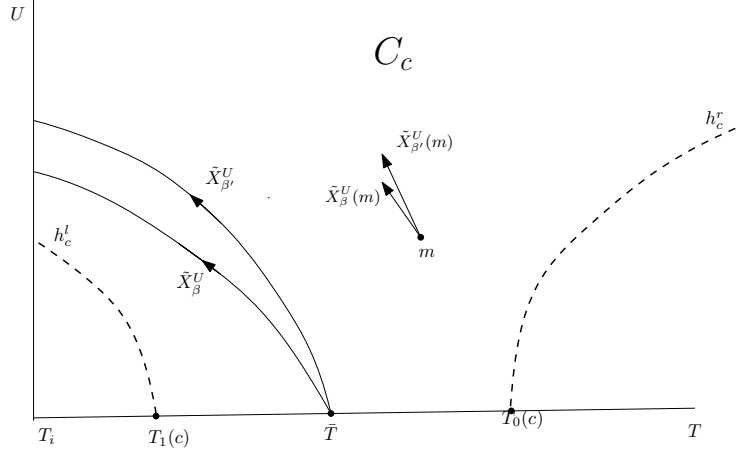


FIGURE 8. Rotating property in function of β with $\beta' > \beta$.

The vector field $\frac{\partial \tilde{X}_{\beta,c}^U}{\partial c}(m) = -T \frac{\partial}{\partial T}$ is transverse to $\tilde{X}_{\beta,c}^U$ on the whole domain Q . Moreover, the pair $(\tilde{X}_{\beta,c}^U(m), \frac{\partial \tilde{X}_{\beta,c}^U}{\partial c}(m))$ has a direct orientation. Then, the family $\tilde{X}_{\beta,c}^U$ has the rotating property in the direct direction on the open connected set Q , in function of the parameter $\varepsilon = c - c_0$ for any $c_0 \in [c^{ej}, +\infty)$. This direct orientation implies that $\frac{\partial \tilde{X}_{\beta,c}^U}{\partial c}(m)$ is oriented as the opposite direction of the Z -axis in comparison to the orbit of $\tilde{X}_{\beta,c}^U$, at any point m of Q .

We consider the trajectory $\gamma_{\beta,c_0}(T)$ of \tilde{X}_{β,c_0}^U starting at any point $(T, 0)$, for $T \geq T_i$. This trajectory is contained in Q and cuts the boundary ∂Q only at the starting point $(T, 0)$. Then, a direct consequence of Lemma 3.6 is the following:

Corollary 3.10. For $T \geq T_i$ and any (β, c) we have that: $\frac{\partial Z}{\partial c}(T, \beta, c) < 0$.

4. BIFURCATION DIAGRAM IN THE (β, c) -SPACE

We can now deduce from the previous results a diagram of bifurcation for the solution.

4.1. The bifurcation curves $\beta = \beta_1(c)$ and $\beta = \beta_0(c)$.

Theorem 4.1. There exists a function $\beta_0(c) : [c^{ej}, +\infty) \rightarrow \mathbb{R}^+$, of class $[\frac{1}{1-\alpha}]$, such that:

- (i) there is a special solution (i.e., a finite-time solution) for $\beta = \beta_0(c)$;
- (ii) there is a non-monotonic solution with a bump for $0 < \beta < \beta_0(c)$.

Proof. Take any $c \geq c^{ej}$. From Proposition 3.2, we know that $Z_0(\beta, c) < 1$ if $\beta > 0$ is small enough. From Proposition 3.9 we know, that $Z_0(\beta, c)$ is of class $[\frac{1}{1-\alpha}]$ with a positive partial derivative in function of β , and from Proposition 3.4 we know that $Z_0(\beta, c) \rightarrow +\infty$ if $\beta \rightarrow +\infty$.

Then, by the implicit function theorem, there exists a unique function $\beta_0(c)$ of class $\left[\frac{1}{1-\alpha}\right]$ such that $Z_0(\beta_0(c), c) = 1$. Clearly, if $0 < \beta < \beta_0(c)$, we have that $Z_0(\beta, c) < 1$ and there is a solution of bump type. \square

Theorem 4.2. (i) Let $c \geq c_* = \frac{T_i^2 + 2q_0}{T_i}$, there is a solution for any $\beta > 0$ and, if $\beta > \beta_0(c)$, this solution is of monotonic type;

(ii) there exists a function $\beta_1(c) : [c^{c^j}, c_*) \rightarrow \mathbb{R}^+$, of class $\left[\frac{1}{1-\alpha}\right]$, with the following properties:

- (a) For all $c \in (c^{c^j}, c_*)$ we have that $\beta_0(c) < \beta_1(c)$ and $\beta_0(c^{c^j}) = \beta_1(c^{c^j})$. We call β^{c^j} this common value;
- (b) for $\beta_0(c) < \beta < \beta_1(c)$, there is a solution of monotonic type;
- (c) there is no solution if $c \in [c^{c^j}, c_*)$ and $\beta \geq \beta_1(c)$.
- (d) $\beta_1'(c) > 0$ for $c \in (c^{c^j}, c_*)$. Moreover $\beta_1(c) \rightarrow +\infty$ when $c \rightarrow c_*$.

Proof. The point (i) is a direct consequence of Lemma 3.1 and the fact that if $\beta > \beta_0(c)$, then $1 < Z_0(\beta, c)$.

To prove the existence of the function $\beta_1(c)$ with properties (a), (b) and (c), we use the same arguments as in Theorem 4.1. That $\beta_0(c) < \beta_1(c)$ for any $c \in (c^{c^j}, c_*)$ comes from the fact that, if β increases, then the point $Z_0(c)$ crosses the value 1 before the point $Z_1(c)$. For $c = c^{c^j}$, we have that $Z_0(c^{c^j}) = Z_1(c^{c^j})$ and then that $\beta_0(c^{c^j}) = \beta_1(c^{c^j})$.

In order to prove the first claim of (d), we use that the function $\beta_1(c)$ is an implicit solution of the equation: $Z_1(\beta_1(c), c) = Z(T_1(c), \beta_1(c), c) = 1$. Differentiating it gives that

$$\frac{\partial Z}{\partial T} T_1'(c) + \frac{\partial Z}{\partial c} + \frac{\partial Z}{\partial \beta} \beta_1'(c) = 0,$$

where the partial derivatives are evaluated at $(T_1(c), \beta_1(c), c)$. We have that $\frac{\partial Z}{\partial T} > 0$, $\frac{\partial Z}{\partial c} < 0$, $\frac{\partial Z}{\partial \beta} > 0$ and $T_1'(c) < 0$. Then $\beta_1'(c) > 0$ for $c \in (c^{c^j}, c_*)$.

We now prove the second claim of (d). Take any value $\beta > \beta^{c^j}$. As $\beta^{c^j} = \beta_1(c^{c^j})$, we know that $Z_1(\beta, c^{c^j}) > 1$. On the other side, we have that $Z_1(\beta, c_*) = 0$. As above, we have that

$$\frac{\partial Z_1}{\partial c} = \frac{\partial Z}{\partial T} T_1'(c) + \frac{\partial Z}{\partial c} < 0.$$

Then, there exists a unique $c_1(\beta)$ such that $\beta_1(c_1(\beta)) = \beta$ (this means that the function $\beta \mapsto c_1(\beta)$ is the inverse of the function $\beta_1(c)$). Now, if $c \in [c_1(\beta), c_*)$ we have that $\beta_1(c) \geq \beta$. As this is true for any $\beta > \beta^{c^j}$, this means that $\beta_1(c) \rightarrow +\infty$ when $c \rightarrow c_*$. \square

4.2. Behaviour near $c = c^{c^j}$. Let us recall that $\beta_0(c^{c^j}) = \beta_1(c^{c^j})$ and that we write β^{c^j} this common value.

Proposition 4.3. *The union of the graphs of β_0 and β_1 with the point (β^{c^j}, c^{c^j}) is a simple curve (B) in the parameter space, of class $\left[\frac{1}{1-\alpha}\right]$, diffeomorphic to \mathbb{R} and tangent to the axis $\{c = c^{c^j}\}$. This contact is quadratic if $\alpha \geq \frac{1}{2}$.*

Proof. As the graphs of β_0 and β_1 are simple curves above for $c > c^{c^j}$, it is sufficient to prove that (B) is also a simple curve in a small neighborhood of the point (β^{c^j}, c^{c^j}) .

The equation of (B) is given by the elimination of T between the two equations:

$$(4.1) \quad \begin{cases} P_c(T) = -cT + \frac{1}{2}T^2 + q_0 = 0, \\ Z(T, \beta, c) - 1 = 0. \end{cases}$$

It follows from Corollary 3.10, applied to the limit case $c = c^{ej}$, that

$$\frac{\partial Z}{\partial \beta}(c^{ej}, \beta, \sqrt{2q_0}) > 0.$$

Then, for $(T, \beta, c) \sim (\sqrt{2q_0}, \beta^{ej}, c^{ej})$, we can solve the second equation for an implicit function $\beta = \beta(T, c)$ with $\beta(c^{ej}, c^{ej}) = \beta^{ej}$, defined in a neighborhood W of $(T, c) = (\sqrt{2q_0}, c^{ej})$. As $\frac{\partial Z}{\partial T} + \frac{\partial Z}{\partial \beta} \frac{\partial \beta}{\partial T} = 0$, we can choose W small enough such that $\frac{\partial Z}{\partial \beta} > 0$ and then such that $\frac{\partial \beta}{\partial T}(T, c) < 0$ on W .

On the other side, it is easy to verify that the first equation defines for $c \geq c^{ej}$ an arc of hyperbola, which is a graph of the function

$$c(T) = \frac{1}{2}T + \frac{q_0}{T}$$

restricted to $T \in [T_i, +\infty)$. This function, $c(T)$, has a minimum at $T = \sqrt{2q_0}$. Finally, (B) near the point (β^{ej}, c^{ej}) is a T -parametrized curve:

$$(4.2) \quad (B) := \begin{cases} c = c(T), \\ \tilde{\beta}(T) = \beta(T, c(T)). \end{cases}$$

This curve passes through the point $(\sqrt{2q_0}, \bar{\beta})$ for $T = \sqrt{2q_0}$. We have that $\tilde{\beta}'(T) = \frac{\partial \beta}{\partial T}(T, c(T)) + \frac{\partial \beta}{\partial c}(T, c(T))c'(T)$. In particular, for $T = \sqrt{2q_0}$, we have that $c'(\sqrt{2q_0}) = 0$ and $\frac{\partial \beta}{\partial T}(\sqrt{2q_0}, \sqrt{2q_0}) < 0$. Then, $\tilde{\beta}'(\sqrt{2q_0}) < 0$, which proves that (B) is a simple curve in a neighborhood of $(\sqrt{2q_0}, \bar{\beta})$.

If $\alpha \geq 2$, all the functions are at least of class C^2 . Then, we can invert the function $\tilde{\beta}(T)$ as a function $T(\beta)$ of class C^2 , such that $T(\beta^{ej}) = \sqrt{2q_0}$ and $T'(\beta^{ej}) < 0$. Locally, the curve (B) is the graph of the function $\tilde{c}(\beta) = \beta c(T(\beta))$. We have that

$$\tilde{c}'(\beta) = c'(T(\beta))T'(\beta) \quad \text{and} \quad \tilde{c}''(\beta) = c''(T(\beta))(T'(\beta))^2 + c'(T(\beta))T''(\beta).$$

For $\beta = \beta^{ej}$, this gives that $\tilde{c}'(T(\beta^{ej})) = 0$. Then,

$$\tilde{c}'(\beta^{ej}) = 0 \quad \text{and} \quad \tilde{c}''(\beta^{ej}) = c''(T(\beta^{ej}))(T'(\beta^{ej}))^2 > 0,$$

which means that the function \tilde{c} has a quadratic minimum at β^{ej} . □

4.3. Behavior of $\beta_0(c)$ for $c \rightarrow +\infty$. In general, little is known about the behavior of the function $\beta_0(c)$ in the large. The simple proof given for $\beta_1(c)$ does not work in an obvious way, since we do not know the sign of the term $\frac{\partial Z}{\partial T}T'_0(c) + \frac{\partial Z}{\partial c}$ for all c . Here, we introduce an additional technical assumption which is obviously verified by the Heaviside function and the Arrhenius law:

Hypothesis (H_∞): *assume that the function $\psi(V) = \varphi(\frac{1}{V})$ is smooth at $V = 0$ with a value $\psi(0) = A > 0$.*

We know that $\beta'_0(c) \rightarrow -\infty$ for $c \rightarrow c^{ej}$ as consequence of Proposition 4.3. The following result is about the asymptotic behavior of $\beta_0(c)$ at infinity:

Proposition 4.4. *Assume that (H_∞) is verified. If $c \rightarrow +\infty$, then $\beta_0(c) \rightarrow +\infty$.*

Proof. The proof is rather long and uses again the theory of slow-fast systems, but now in a slightly deeper way than in Subsection 2.2 for $\beta \rightarrow 0$. In order to use [7], we need to have C^∞ (smooth) differential systems. Then, we choose any δ such that $0 < \delta < 1$, and we restrict $\tilde{X}_{\beta,c}$ to $Q_\delta = \{T \geq T_i \mid Z \geq \delta\}$. Clearly $\tilde{X}_{\beta,c}$ is smooth on Q_δ . We will proceed in several steps.

Step 1: Reduction to the search of solutions with a bump. We recall that any orbit (image of a trajectory, forgetting the integration time) of $-\tilde{X}_{\beta,c}$ in Q_δ , starting at a point of $\{T = T_i\}$ is a graph in Z , in particular the orbit $\Gamma(\beta, c)$ starting at the point $(T_i, 1)$ is a graph $T = \gamma(Z, \beta, c)$ over $[\delta, 1]$ with $\gamma(1, \beta, c) = T_i$.

The main result of this subsection is the following lemma:

Lemma 4.5. *For any $\beta > 0$, there exists a $c(\beta)$ such that, if $c > c(\beta)$, then the orbit $\Gamma(\beta, c)$ of $-\tilde{X}_{\beta,c}$ starting at $(T_i, 1)$ is of bump type.*

The next steps are devoted to the proof of Lemma 4.5. To complete Step 1, let us show that Lemma 4.5 implies Proposition 4.4: Take any $\beta > 0$, by definition of $\beta_0(c)$, for each $c > c(\beta)$ we have that $\beta_0(c) \geq \beta$. In other words, *for any $\beta > 0$ there exists a $c(\beta)$ such that $c > c(\beta)$ implies that $\beta_0(c) > \beta$* . This means that $\beta_0(c) \rightarrow +\infty$ if $c \rightarrow +\infty$.

Step 2: $\tilde{X}_{\beta,c}$ as a slow-fast system in the small parameter $\varepsilon = \frac{1}{c}$. As we want to consider $c \rightarrow +\infty$, it is convenient to introduce the small positive parameter $\varepsilon = \frac{1}{c} \rightarrow 0_+$ and the slow fast system:

$$(4.3) \quad X_{\beta,\varepsilon} = -\frac{1}{c}\tilde{X}_{\beta,c} := \begin{cases} T' = T - \varepsilon(\frac{1}{2}T^2 + q_0(1 - Z)), \\ Z' = -\varepsilon\beta\varphi(T)Z^\alpha. \end{cases}$$

The division of $\tilde{X}_{\beta,c}$ by c is equivalent to changing the time τ by the time $s = c\tau$. The limit equation is the trivial vector field $T \frac{\partial}{\partial T}$ which has no zero. But it will be interesting to consider the behavior of trajectories of $X_{\beta,\varepsilon}$ for $T \rightarrow +\infty$.

Step 3: Looking near $T = +\infty$. To overcome the problems associated with non-compactness, we compactify $X_{\beta,\varepsilon}$ in the T -direction by introducing the coordinate $V = \frac{1}{T}$. In the chart (U, V) , the system $X_{\beta,\varepsilon}$ reads:

$$(4.4) \quad X_{\beta,\varepsilon} := \begin{cases} V' = -V + \varepsilon(\frac{1}{2} + q_0(1 - Z)V^2), \\ Z' = -\varepsilon\beta\varphi(\frac{1}{V})Z^\alpha. \end{cases}$$

The domain Q_δ given by $Q_\delta = \{0 < V < V_i = \frac{1}{T_i}\}$, $Z \geq \delta$ is compactified for $T \rightarrow +\infty$ by the smooth extension to $V = 0$. The orbit $\Gamma(\beta, c)$ is now called $\Gamma(\beta, \varepsilon)$. It is a graph $V = \tilde{\gamma}(Z, \beta, \varepsilon)$ over the Z -interval $[\delta, 1]$. As we go from $\gamma(Z, \beta, c)$ to $\tilde{\gamma}(Z, \beta, \varepsilon)$ by a diffeomorphism of the target space, the critical points are preserved and $\Gamma(\beta, c)$ *will be a bump type solution if there exists a $\bar{Z} \in (\delta, 1)$ such that $\frac{\partial \tilde{\gamma}}{\partial Z}(\bar{Z}, \beta, \varepsilon) = 0$* . The hypothesis (H_∞) allows to apply the theory of slow fast systems in a neighborhood of the axis $\{V = 0\}$.

Step 4: Center manifold. We consider $X_{\beta,\varepsilon}$ in the chart (V, Z) which covers the whole domain Q_δ . For $\varepsilon = 0$ and any β , the vector field $X_{\beta,\varepsilon}$ has a normally hyperbolic line of zeros $\{V = 0\}$ and then is a slow-fast system of class C^∞ . By adding the trivial equations $\dot{\varepsilon} = 0, \dot{\beta} = 0$, we can consider $X_{\beta,\varepsilon}$ as a C^∞ -differential system in four coordinates $(Z, V, \beta, \varepsilon)$. Along the critical surface, $\{V = \varepsilon = 0\}$, this 4-dimensional vector field has at each point m an hyperbolic attracting direction, the V -axis with eigenvalue -1 , and a 3-dimensional eigenspace $E_0(m)$ parallel to $\{V = 0\}$, with eigenvalue 0. The slow dynamics is defined along the critical line in the slow time τ by the equation $\frac{dZ}{d\tau} = -\beta AZ^\alpha$. This slow dynamics has no singularity as $\beta A > 0$ and $Z \geq \delta > 0$.

The Fenichel theory (see [11]) shows existence of *center manifolds* along normally hyperbolic pieces of the critical set for general slow-fast differentiable systems. Here, we will use the formulation of the Fenichel theory as in [7], which is specific to the smooth slow-fast systems in *dimension 2* and where the existence of smooth center manifolds is proved *when the slow dynamics has no singularities*.

General results of [7] can be translated into the following formulations adapted to our case:

Theorem 4.6. *We consider the slow-fast system $X_{\beta,\varepsilon}$ (4.4). Let Z_1 such that $\delta < Z_1 < 1$ and $[b_0, b_1]$ an interval in the β -axis, with $0 < b_0 < b_1$. For $\varepsilon_0 > 0$ small enough, there exists a function*

$$V = f(Z, \beta, \varepsilon) : [\delta, Z_1] \times [b_0, b_1] \times [0, \varepsilon_0] \rightarrow \mathbb{R},$$

of class C^∞ , with $f(Z, \beta, 0) \equiv 0$, whose graph is an hypersurface W tangent to $X_{\beta,\varepsilon}$, called center manifold of the system, along the critical set $C = [\delta, Z_1] \times [b_0, b_1] \times \{0\}$. At each point $m \in C$, this center manifold is tangent to the eigenspace $E_0(m)$. The center manifold is not unique: there exists a $M > 0$ (depending on δ, Z_1) such that if f_1 and f_2 are functions defining two center manifolds, we have that:

$$|f_1(Z, \beta, \varepsilon) - f_2(Z, \beta, \varepsilon)| \leq e^{-\frac{M}{\varepsilon}}$$

for $(Z, \beta, \varepsilon) \in [\delta, Z_1] \times [b_0, b_1] \times (0, \varepsilon_0]$. One says that the two center manifolds have an exponentially flat contact. A consequence is that there exists a unique formal center manifold, as all center manifolds along have the same formal Taylor series along the critical set C .

All center manifolds attract exponentially the nearby trajectories. More specifically, another result that resulted from [7], in a form adapted to our case, is the following:

Theorem 4.7. *We consider the slow-fast system $X_{\beta,\varepsilon}$ (4.4). Let be Z_1, δ, b_0, b_1 as in Theorem 4.6. For $\varepsilon_0 > 0$ small enough, if*

$$V = f(Z, \beta, \varepsilon) : [\delta, Z_1] \times [b_0, b_1] \times [0, \varepsilon_0] \rightarrow \mathbb{R}$$

is the graph of a smooth center manifold along I , we have that:

$$|f(Z, \beta, \varepsilon) - \tilde{\gamma}(Z, \beta, \varepsilon)| \leq e^{-\frac{M}{\varepsilon}}$$

for $(Z, \beta, \varepsilon) \in [\delta, Z_1] \times [b_0, b_1] \times (0, \varepsilon_0]$, with the same constant M as in Theorem 4.6.

Step 5: Finite expansion of center manifold. It is easy to compute the following finite ε -expansion of a function $V = f(Z, \beta, \varepsilon)$ defining a central manifold:

Lemma 4.8. *Let $V = f(Z, \beta, \varepsilon)$ be the graph of a center manifold of $X_{\beta,\varepsilon}$ along C . Then, we have that*

$$f(Z, \beta, \varepsilon) = \frac{\varepsilon}{2} + \frac{q_0(1-Z)}{4}\varepsilon^3 + O(\varepsilon^4),$$

uniformly in $(Z, \beta) \in [\delta, Z_1] \times [b_0, b_1]$.

Proof

The tangent vector to the graph of f at the point (f, Z) is equal to $\frac{\partial}{\partial Z} + \frac{\partial f}{\partial Z} \frac{\partial}{\partial V}$. We have to write that this vector is proportional to the vector $X_{\beta,\varepsilon}(f, Z)$. This gives

$$(4.5) \quad \frac{\partial f}{\partial Z} = \frac{-f + \varepsilon[\frac{1}{2} + q_0(1-Z)f^2]}{-\varepsilon\beta\psi(f)Z^\alpha}.$$

Consider the expansion of f at order 1 in ε : $f(Z, \beta, \varepsilon) = \varepsilon U_1(Z, \beta) + O(\varepsilon^2)$. We have that $\frac{\partial f}{\partial Z}(Z, \beta, \varepsilon) = \varepsilon \frac{\partial U_1}{\partial Z}(Z, \beta) + O(\varepsilon^2)$. Plugging these expansions in (4.5) gives that:

$$\varepsilon \frac{\partial U_1}{\partial Z} + O(\varepsilon^2) = \frac{-U_1 + \frac{1}{2}}{-\beta A} + O(\varepsilon).$$

Taking $\varepsilon = 0$, it comes that $U_1 = \frac{1}{2}$. Then, $f = \frac{\varepsilon}{2} + \varepsilon^2 U_2(Z, \beta) + O(\varepsilon^3)$ and $\frac{\partial f}{\partial Z} = \varepsilon^2 \frac{\partial U_2}{\partial Z} + O(\varepsilon^3)$. Using these expansions in (4.5),

$$\varepsilon^2 \frac{\partial U_2}{\partial Z} + O(\varepsilon^3) = \frac{-\frac{\varepsilon}{2} - \varepsilon^2 U_2 + O(\varepsilon^3) + \varepsilon(\frac{1}{2} + O(\varepsilon^2))}{-\varepsilon \beta (A + O(\varepsilon)) Z^\alpha}.$$

This implies that $U_2 = O(\varepsilon)$. Again, taking $\varepsilon = 0$, we obtain that $U_2 = 0$. Finally, $f(Z, \beta, \varepsilon)$ reads $f(Z, \beta, \varepsilon) = \frac{\varepsilon}{2} + U_3(Z, \beta)\varepsilon^3 + O(\varepsilon^4)$ and (4.5) yields

$$\varepsilon^3 \frac{\partial U_3}{\partial Z} + O(\varepsilon^4) = \frac{-\frac{\varepsilon}{2} - \varepsilon^3 U_3 + \varepsilon(\frac{1}{2} + \frac{q_0(1-Z)}{4}\varepsilon^2) + O(\varepsilon^4)}{-\varepsilon \beta (A + O(\varepsilon)) Z^\alpha},$$

which in turn implies that $\varepsilon \frac{\partial U_3}{\partial Z} = \frac{-U_3 + \frac{q_0(1-Z)}{4}}{\beta A Z^\alpha} + O(\varepsilon)$. For $\varepsilon = 0$, $U_3 = \frac{q_0(1-Z)}{4}$. \square

Step 6: Proof of Lemma 4.5. It follows from Theorem 4.7 and Lemma 4.8 that :

$$\tilde{\gamma}(Z, \beta, \varepsilon) = \frac{\varepsilon}{2} + \frac{q_0(1-Z)}{4}\varepsilon^3 + O(\varepsilon^4),$$

uniformly in $(Z, \beta) \in [\delta, Z_1] \times [b_0, b_1]$. As a consequence we have that $\frac{\partial \tilde{\gamma}}{\partial Z}(Z, \beta, \varepsilon) < 0$, for $\varepsilon > 0$ small enough, uniformly in $(Z, \beta) \in [\delta, Z_1] \times [b_0, b_1]$. On the other side, as the limit vector field for $\varepsilon \rightarrow 0$ is horizontal, we have that $\frac{\partial \tilde{\gamma}}{\partial Z}(1, \beta, \varepsilon) \rightarrow +\infty$ for $\varepsilon \rightarrow 0$, uniformly in $\beta \in [b_0, b_1]$. It follows that there exists a value $\bar{Z}(\beta) \in]Z_1, 1[$ where $\frac{\partial \tilde{\gamma}}{\partial Z}(\bar{Z}(\beta), \beta, \varepsilon) = 0$, if $\varepsilon > 0$ small enough, uniformly in $\beta \in [b_0, b_1]$. This proves the statement of Lemma 4.5.

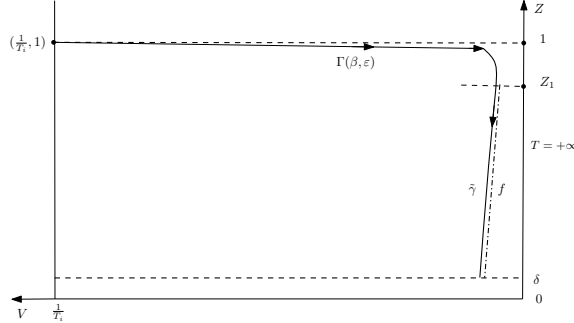


FIGURE 9. $X_{\beta, \varepsilon}$ for ε small

5. NUMERICAL RESULTS

To better understand the Majda-Rosales model with fractional order and confirm our theoretical results, we perform some numerical computations in view of the bifurcation diagram, starting from the vector field (2.2).

First, we focus on the Heaviside function $\varphi(T) = H(T - T_i)$, try to find an equivalent form of the solution of the system (2.2), and plot the bifurcation diagram using Maple. Then we move on to the Arrhenius law $\varphi(T) = H(T - T_i) \exp(-\frac{T}{T_0})$, using some qualitative results discussed in the previous chapters, we design numerical methods to explore and confirm the specific properties of the respective bifurcation diagrams.

Two methods are implemented: an analytical method (see Appendix A) and a shooting method (see Appendix B). For the sake of simplicity, the analytical method will be limited to the Heaviside law in the special case $\alpha = 0.5$. The shooting method will be presented for the Heaviside function and the Arrhenius law, the Heaviside function being clearly a simplification as mentioned earlier.

5.1. Analytical method for Heaviside law. First, we try to derive an expression that connects the initial condition $(U(0), T(0)) = (\frac{1}{1-\alpha}, T_i)$ with the final condition $(U(-\ell'), T(-\ell')) = (0, T_0(c))$ (or $(U(-\ell'), T(-\ell')) = (0, T_1(c))$) while characterizing the dependence on the parameters c and β . After integrating the second ODE in the system (2.2) with the initial condition $U(0) = \frac{1}{1-\alpha}$, we have

$$(5.1) \quad U(\tau) = \beta\tau + \frac{1}{1-\alpha}, \quad \ell' = \frac{1}{\beta(1-\alpha)}.$$

This immediately decouples the system as a Riccati equation

$$(5.2) \quad \dot{T} = -cT + \frac{1}{2}T^2 + q_0 \left(1 - (1-\alpha)^{\frac{1}{1-\alpha}} \left(\beta\tau + \frac{1}{1-\alpha} \right)^{\frac{1}{1-\alpha}} \right),$$

with initial condition $T(0) = T_i$.

Several types of solutions can be observed by applying the Runge-Kutta 4/5 method to (5.2) for different values of the parameter $\beta > 0$ and a fixed value of the parameter $c > c^{cj}$, see Figures 10 to 12.

As announced, for simplicity we fix $\alpha = 0.5$, $q_0 = 2$, and $T_i = 0.5$ in this section. Then, we use Maple's ODE solver `dsolve` to derive an equivalent form of the solution for (5.2) with the initial condition $T(0) = T_i$ and then derive an equation $T(-\ell') - T_0(c) = 0$ (see (A.3)) by plugging the final conditions into the latter. Finally, using Maple's implicit function tool `implicitplot` (see [12]) on the formula (A.2)), with the range $\beta = 0.015$, $c = 2.5$ and the grid option `gridrefine = 5`, we generate a visual representation of the local implicit function for the curve $\beta_0(c)$ in the parameter space. Similarly, the result of the equation $T(-\ell') - T_1(c) = 0$ is displayed in (A.4). Finally repeating the previous steps, the bifurcation diagram is displayed as Figure 13.

We observe that the bifurcation diagram generated by Maple agrees with the qualitative results:

- (i) the curves $\beta_0(c)$ and $\beta_1(c)$ are smooth, they merge at the critical point (β^{cj}, c^{cj}) of the curve (B) , see Proposition 4.3;

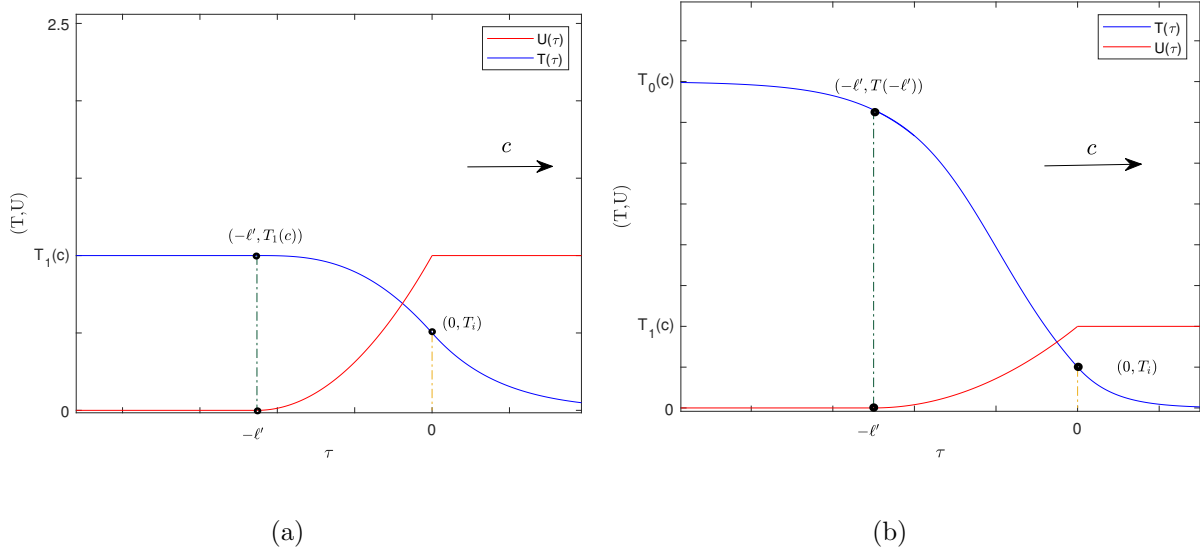


FIGURE 10. Profiles of solutions of the vector field (1.21), extended to the entire real line, with values of parameters $\alpha = 0.5$, $q_0 = 2$, $T_i = 0.5$, $c = 2.5$. (a) $\beta = 1.7675$, weak reactive waves of special type; (b) $\beta = 0.8$, strong reactive wave with monotonic type with velocity c . The ignition temperature is reached at $\tau = 0$ and the free interface is at $\tau = -\ell'$.

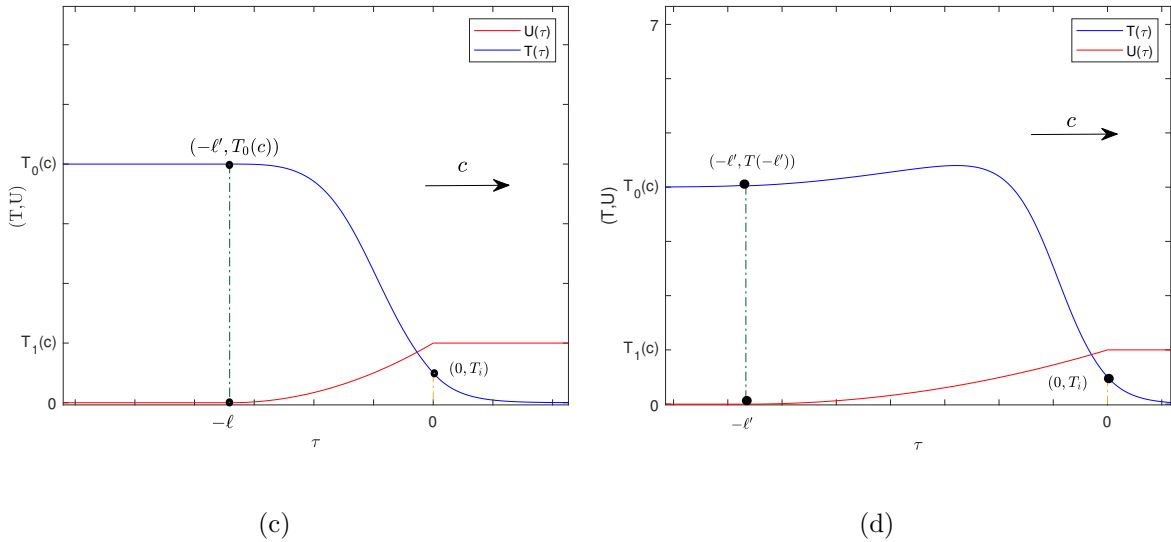


FIGURE 11. Profiles of solutions of the vector field (1.21), extended to the entire real line, with values of parameters $\alpha = 0.5$, $q_0 = 2$, $T_i = 0.5$, $c = 2.5$. (c) $\beta = 0.582$, strong reactive wave of special type; (d) $\beta = 0.4$, strong reactive wave with a bump.

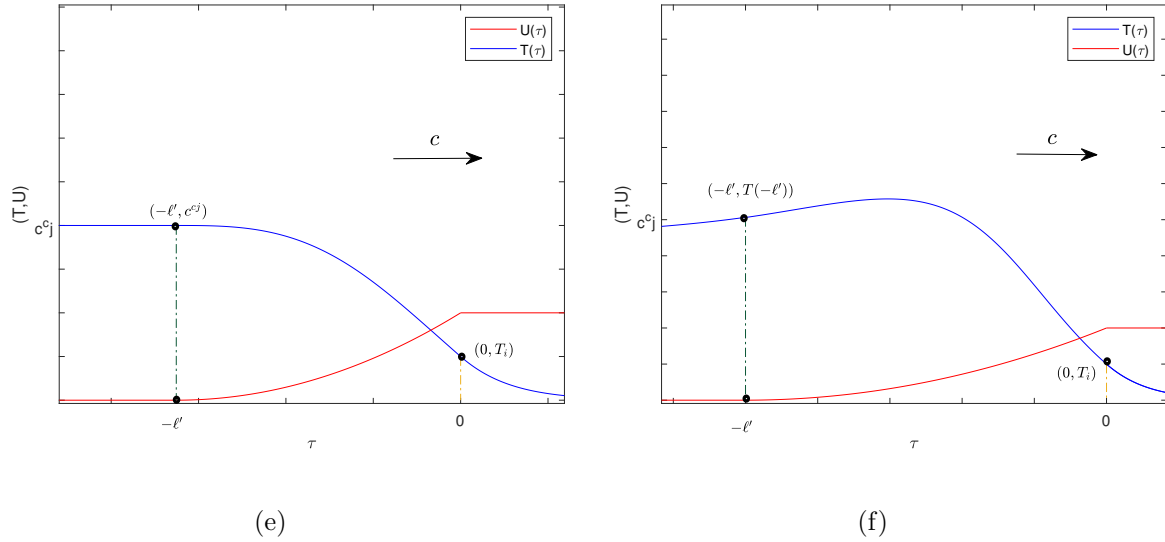


FIGURE 12. Profiles of solutions of the vector field (1.21), extended to the entire real line, with values of parameters $\alpha = 0.5$, $q_0 = 2$, $T_i = 0.5$, $c = 2$. (e) $\beta = 0.615$, CJ reactive wave of special type. (f) $\beta = 0.4$, CJ reactive wave with a bump (combustion spike).

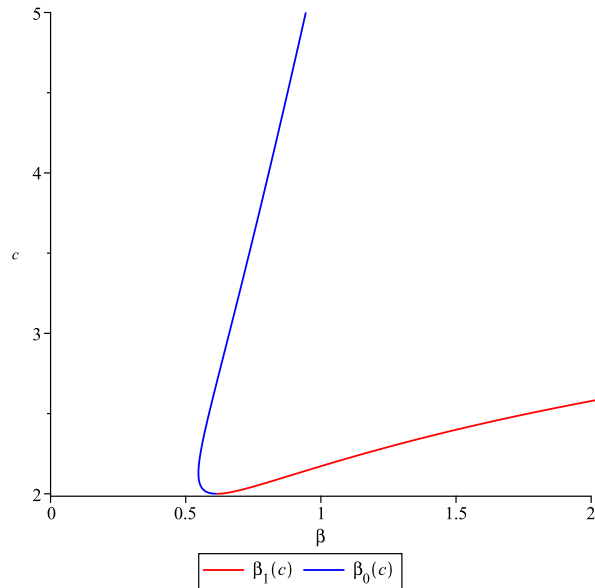


FIGURE 13. Bifurcation diagram in the case of Heaviside function with parameter values $\alpha = 0.5$, $q_0 = 2$, $T_i = 0.5$.

- (ii) we also observe a local extremum of the function $\beta_0(c)$ for $c > c^{c_j}$, see Figure 14, namely a turning point $(\bar{\beta}, \bar{c})$ which seemingly is unique.

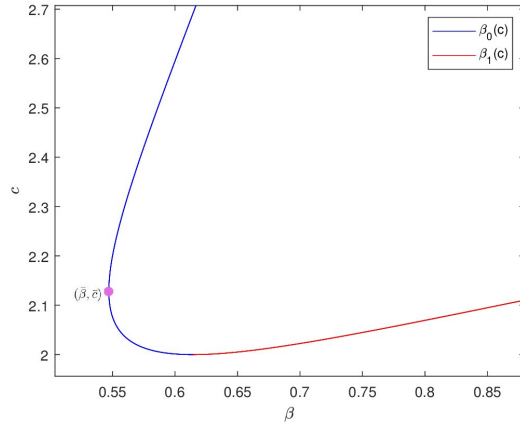
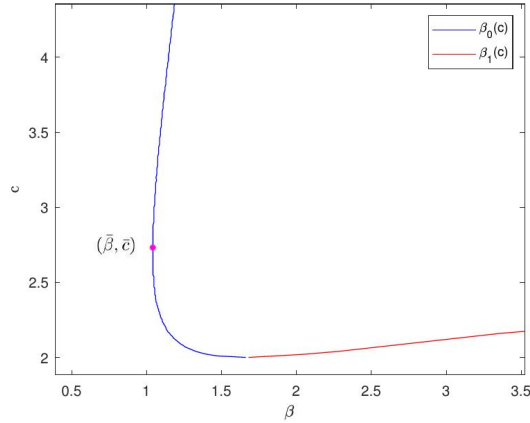
FIGURE 14. Enlargement of Fig. 13 around the turning point $(\bar{\beta}, \bar{c})$.

FIGURE 15. Enlargement of Fig. 16 in a neighborhood of the turning point.

Remark 5.1. *The accuracy of the computation of the numerical value of the critical point (β^{c^j}, c^{c^j}) may be improved as follows: plugging $c = c^{c^j}$ into (A.3) yields the formula:*

$$(5.3) \quad T(-\ell') - c^{c^j} = \frac{3\beta\Gamma\left(\frac{3}{4}\right)^2 \sqrt{\frac{1}{\beta}} \left(\frac{3}{4}I_{-\frac{1}{4}}\left(\frac{1}{\beta}\right) - I_{\frac{3}{4}}\left(\frac{1}{\beta}\right) \right)}{\pi \left(\frac{9}{8}I_{\frac{1}{4}}\left(\frac{1}{\beta}\right) - \frac{3}{2}I_{-\frac{3}{4}}\left(\frac{1}{\beta}\right) \right)} = 0,$$

where $I_\nu(z)$ is a Bessel function of the first kind, $\Gamma(u)$ the Gamma function. Using Maple, formula (5.3) provides the following approximated value: $\beta^{c^j} \approx 0.614452673918923$.

5.2. Numerical shooting method for Arrhenius kinetics. A number of problems arise where the position of the free interface cannot be determined due to the inability to decouple the system when considering the Arrhenius function. To numerically simulate the bifurcation curves $\beta_0(c)$ and $\beta_1(c)$, we employ a shooting-based numerical scheme. Specifically, we discretize the parameter space with uniform meshes, and for each fixed parameter c , we determine the

corresponding β value by exploiting the monotonicity of the transition mappings (see proposition 3.9), combined with a highly accurate Runge-Kutta method for solving the ODE system (see, e.g., [10, 15, 23]). The detailed numerical procedure is presented in Appendix B, following the implementation of the numerical method. The bifurcation diagram is shown in Figure 16.

Finally, we study the influence of the parameter α on the curves $\beta_0(c)$ and $\beta_1(c)$ in Figure 19.

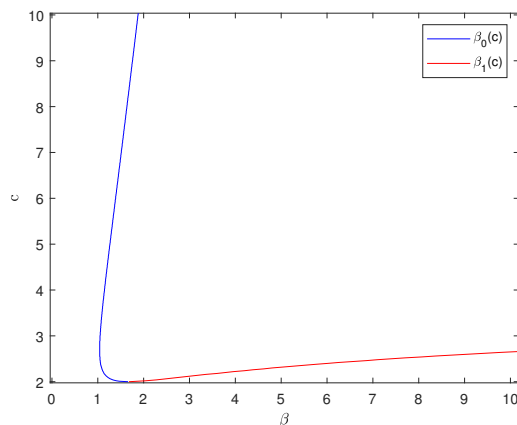


FIGURE 16. Bifurcation diagram for Arrhenius kinetics with parameter values: $\alpha = 0.5$, $T_a = 1$, $q_0 = 2$, $T_i = 0.5$.

5.3. Validation. The validation method employed is predicated on the observation that the numerical shooting is evidently applicable to the Heaviside function.

In order to compare the results obtained by the two methods, we substitute $\bar{\ell}$ with $\ell' = \frac{1}{\beta(1-\alpha)}$ in step (4) of Appendix B. Figure 17 showcases our results which exhibit a nearly complete overlap of the two curves produced by the two methods, which therefore give similar results whenever they are applicable.

An other observation is the consistent behavior of the bifurcation curves $\beta_0(c)$ and $\beta_1(c)$ across different modeling scenarios (Heaviside and Arrhenius). This similarity suggests that the underlying dynamics of the system is robust to variations in the functional form of the reaction rate.

Finally, we point out the flexibility of the shooting method which allows for easy adjustments to the parameter intervals. This makes it easy to thoroughly explore the bifurcation landscape. Future research will focus on the influence of additional parameters on the behavior of the system, extending the investigation into the parameter space to uncover more complex dynamic features.

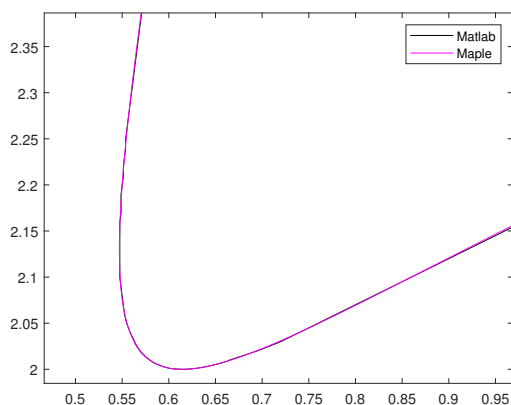


FIGURE 17. Comparison of the two methods.

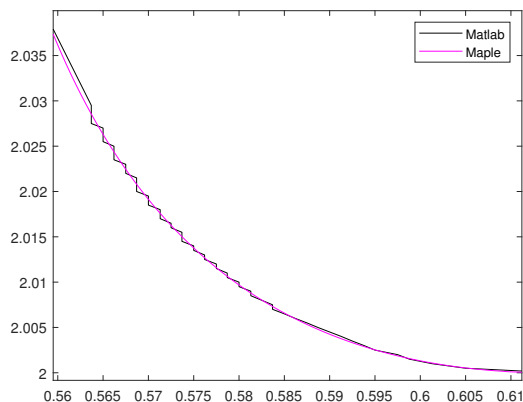


FIGURE 18. Comparison of the two methods (enlargement).

1. ACKNOWLEDGMENTS

The authors are appreciative of the fruitful discussions with Prof. Victor Roytburd. They also wish to thank Prof. Hanchun Yang for bringing reference [17] to their attention and providing sound advice. C.-M. B. greatly acknowledges Prof. Mei Ming and the Department of Mathematics and Statistics of Yunnan University for their warm hospitality during his visiting positions in 2023 and 2024. This project was supported by the National Natural Science Foundation of China (No.12222116). The Institut de Mathématiques de Bourgogne receives support from EPHI Graduate School (contract ANR-17-0002).

REFERENCES

- [1] I. Bendixson, *Sur les courbes définies par des équations différentielles*, Acta Math. **24** (1901), 1–88.
- [2] I. Brailovsky, P.V. Gordon, L. Kagan, and G.I. Sivashinsky, *Shape-thermal instabilities in premixed flames: stepwise ignition-temperature kinetics*, Combust. Flame **162** (2015), 2077–2086.

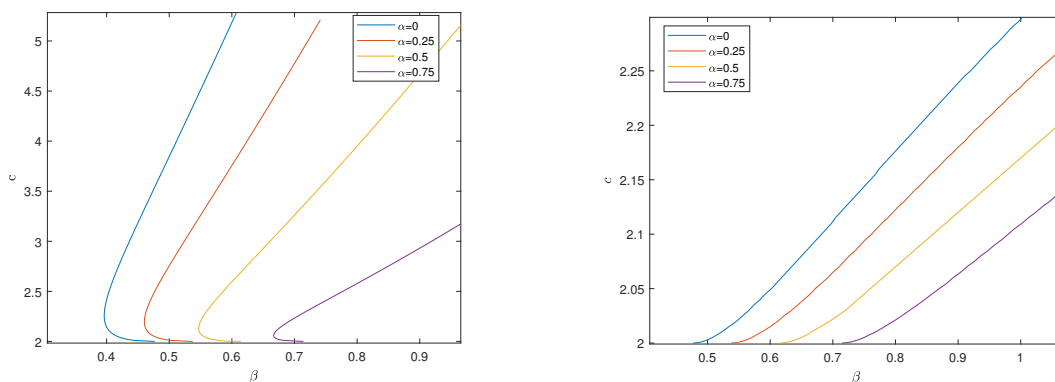


FIGURE 19. Effect of parameter α on the curve $\beta_0(c)$ (left) and on the curve $\beta_1(c)$ (right). Here, $T_a = 1$, $q_0 = 2$, $T_i = 0.5$.

- [3] C.-M. Brauner, R. Roussarie, P. Shang, and L. Zhang, *Existence of a traveling wave solution in a free interface problem with fractional order kinetics*, J. Differ. Equations **281** (2021), 105–147.
- [4] J.D. Buckmaster and G.S.S. Ludford, *Theory of Laminar Flames*, Cambridge University Press, 1982.
- [5] E.A. Coddington and N. Levinson, *Theory of ordinary differential equations* (Chapters 13–17), McGraw-Hill, New York, 1955.
- [6] P. Colella, A. Majda, and V. Roytburd, *Theoretical and numerical wave structure for reacting shock waves*, SIAM J. Sci. Stat. Comput. **7** (1986), 1059–1080.
- [7] F. Dumortier, P. De Maesschalck, and R. Roussarie, *Canard Cycles: From Birth to Transition*, Ergebnisse Math. Grenzgebiete **73**, Springer, 2022.
- [8] F. Dumortier, J. Llibre, and J.C. Artés, *Qualitative Theory of Planar Differentiable Systems*, Universitext, Springer-Verlag, 2006.
- [9] G.F. Duff, *Limit cycles and rotated vector fields*, Ann. Math. **57**, no. 2 (1953), 15–31.
- [10] E.J. Doedel, *AUTO: A program for the automatic bifurcation analysis of autonomous systems*, Congr. Numerantium **30** (1981), 265–284.
- [11] N. Fenichel, *Geometric singular perturbation theory for ordinary differential equations*, J. Differ. Equations **31**, no. 1 (1979), 53–98.
- [12] A. Heck, *Introduction to Maple*, Springer, New York, 2003.
- [13] J. Hendricks, J. Humpherys, G. Lyng, and K. Zumbrun, *Stability of viscous weak detonation waves for Majda’s model*, J. Dyn. Differential Equations **27**, no. 2 (2015), 237–260.
- [14] J. Humpherys, G. Lyng, and K. Zumbrun, *Stability of viscous detonations for Majda’s model*, Phys. D **259** (2013), 63–80.
- [15] H.B. Keller, *Numerical Methods for Two-Point Boundary-Value Problems*, Dover Publications, 1992.
- [16] S. Lefschetz, *Differential Equations: Geometric Theory*, 2nd ed., Dover Publications, New York, 1977.
- [17] T. Li, *On the initiation problem for a combustion model*, J. Differential Equations **112** (1992), 351–373.
- [18] A. Majda, *A qualitative model for dynamic combustion*, SIAM J. Appl. Math. **41**, no. 1 (1981), 70–93.
- [19] A. Majda and V. Roytburd, *Numerical study of the mechanisms for initiation of reacting shock waves*, SIAM J. Sci. Stat. Comput. **11** (1990), 950–974.
- [20] W.N. Mathews, M.A. Esrick, Z.Y. Teoh, and J.K. Freericks, *A physicist’s guide to the solution of Kummer’s equation and confluent hypergeometric functions*, Condens. Matter Phys. **25**, no. 3 (2022), 33203, doi:10.5488/CMP.25.33203.
- [21] H. Poincaré, *Sur les courbes définies par des équations différentielles*, J. Math. Pures Appl. Ser. 3 **7** (1881) and *Œuvres de Henri Poincaré, tomes I-XI*, Gauthier-Villars (new impression 1950–1965).
- [22] J. Palis and W. De Melo, *Geometric Theory of Dynamical Systems*, Springer, Berlin-Heidelberg-New York, 1982.
- [23] L.F. Shampine and M.W. Reichelt, *The MATLAB ODE Suite*, SIAM J. Sci. Comput. **18** (1997), 1–22.

- [24] R.R. Rosales and A. Majda, *Weakly nonlinear detonation waves*, SIAM J. Appl. Math. **43**, no. 5 (1983), 1086–1118.
- [25] V. Roytburd, *private communication to T. Li (1992)*.
- [26] A. Szepessy, *Dynamics and stability of a weak detonation wave*, Commun. Math. Phys. **202**, no. 3 (1999), 547–569.

APPENDIX A. SOLVING RICCATI EQUATION ($\alpha = 0.5$).

This first appendix shows the results of the calculation of the Riccati equation (5.2) when the special value $\alpha = 0.5$ is considered.

We recall that the Kummer's function $M(a; b; z)$ is a generalized hypergeometric series, often referred to as the confluent hypergeometric function of the first kind, given by

$$(A.1) \quad M(a; b; z) = {}_1F_1(a, b, z) = \sum_{n=0}^{\infty} \frac{(a)_n z^n}{(b)_n n!},$$

where $(a)_n$ is the Pochhammer symbol (see, e.g. [20]).

The equivalent form of the solution of the Riccati equation with the initial condition $T(0) = T_i$ is displayed as follows:

$$\begin{aligned} T(\tau) = & \left[-3(\beta\tau + 2)^2 \left(\beta M \left(\frac{2\beta\sqrt{q_0} + \sqrt{2}(c^2 - 2q_0)}{8\beta\sqrt{q_0}}; \frac{1}{2}; \frac{\sqrt{2}\sqrt{q_0}}{\beta} \right) \left(-\frac{2\sqrt{2}q_0^{\frac{3}{2}}}{3} \right. \right. \right. \\ & + \left. \left. \left((c - T_i)\beta + \frac{c^2}{3} \right) \sqrt{2}\sqrt{q_0} + 2q_0\beta + \frac{(c - T_i)(c^2 - 2q_0)}{3} \right) - 2 \left(-\frac{4\beta\sqrt{2}q_0^{\frac{3}{2}}}{3} + \frac{2\beta c^2\sqrt{2}\sqrt{q_0}}{3} \right. \right. \\ & \left. \left. + q_0\beta^2 + \frac{(c^2 - 2q_0)^2}{6} \right) M \left(\frac{10\beta\sqrt{q_0} + \sqrt{2}(c^2 - 2q_0)}{8\beta\sqrt{q_0}}; \frac{3}{2}; \frac{\sqrt{2}\sqrt{q_0}}{\beta} \right) \right) \\ & M \left(\frac{14\beta\sqrt{q_0} + \sqrt{2}(c^2 - 2q_0)}{8\beta\sqrt{q_0}}; \frac{5}{2}; \frac{\sqrt{2}\sqrt{q_0}(\beta\tau + 2)^2}{4\beta} \right) + 3(\beta((\tau^2(c - T_i)\beta^2 + (-4 \\ & + (6c - 4T_i)\tau)\beta + 8c - 4T_i)\sqrt{2}\sqrt{q_0} + 2q_0\beta^2\tau^2 + ((-2cT_i + 2c^2 + 8q_0)\tau - 4c + 4T_i)\beta \\ & + 4c^2 - 4cT_i + 8q_0) M \left(\frac{2\beta\sqrt{q_0} + \sqrt{2}(c^2 - 2q_0)}{8\beta\sqrt{q_0}}; \frac{1}{2}; \frac{\sqrt{2}\sqrt{q_0}}{\beta} \right) \\ & - 2 \left(-\sqrt{2}(\beta\tau + 2)^2 q_0^{\frac{3}{2}} + \frac{((c^2\tau^2 + 2c\tau - 4)\beta^2 + (4c^2\tau + 4c)\beta + 4c^2)\sqrt{2}\sqrt{q_0}}{2} + \beta^3 q_0 \tau^2 \right. \\ & \left. + 4q_0\beta^2\tau + (c(c^2 - 2q_0)\tau - 2c^2 + 8q_0)\beta + 2c^3 - 4cq_0 \right) \\ & M \left(\frac{10\beta\sqrt{q_0} + \sqrt{2}(c^2 - 2q_0)}{8\beta\sqrt{q_0}}; \frac{3}{2}; \frac{\sqrt{2}\sqrt{q_0}}{\beta} \right) \\ & \left. \beta M \left(\frac{6\beta\sqrt{q_0} + \sqrt{2}(c^2 - 2q_0)}{8\beta\sqrt{q_0}}; \frac{3}{2}; \frac{\sqrt{2}\sqrt{q_0}(\beta\tau + 2)^2}{4\beta} \right) - 6(\beta\tau + 2) \left(\beta \left(2\sqrt{2}q_0^{\frac{3}{2}} \right. \right. \right. \\ & \left. \left. + (\beta^2 + (-c + T_i)\beta - c^2)\sqrt{2}\sqrt{q_0} + (c^2 - 4q_0)\beta - (c - T_i)(c^2 - 2q_0) \right) \right) \end{aligned}$$

$$\begin{aligned}
& M\left(\frac{6\beta\sqrt{q_0} + \sqrt{2}(c^2 - 2q_0)}{8\beta\sqrt{q_0}}; \frac{3}{2}; \frac{\sqrt{2}\sqrt{q_0}}{\beta}\right) + 2\left(-\frac{4\beta\sqrt{2}q_0^{\frac{3}{2}}}{3} + \frac{2\beta c^2\sqrt{2}\sqrt{q_0}}{3} + q_0\beta^2\right. \\
& \left. + \frac{(c^2 - 2q_0)^2}{6}\right) M\left(\frac{14\beta\sqrt{q_0} + \sqrt{2}(c^2 - 2q_0)}{8\beta\sqrt{q_0}}; \frac{5}{2}; \frac{\sqrt{2}\sqrt{q_0}}{\beta}\right) \\
& M\left(\frac{10\beta\sqrt{q_0} + \sqrt{2}(c^2 - 2q_0)}{8\beta\sqrt{q_0}}; \frac{3}{2}; \frac{\sqrt{2}\sqrt{q_0}(\beta\tau + 2)^2}{4\beta}\right) + 6\left(\beta\left(\sqrt{2}(\tau\beta^2 + (2 + (-c\right. \right. \\
& \left. \left. + T_i)\tau)\beta - 4c + 2T_i)\sqrt{q_0} + (-2q_0\tau + 2c)\beta - 2c^2 + 2cT_i - 4q_0\right)\right. \\
& M\left(\frac{6\beta\sqrt{q_0} + \sqrt{2}(c^2 - 2q_0)}{8\beta\sqrt{q_0}}; \frac{3}{2}; \frac{\sqrt{2}\sqrt{q_0}}{\beta}\right) + 2\left(-\frac{\sqrt{2}(\beta\tau + 2)q_0^{\frac{3}{2}}}{3}\right. \\
& \left. + \frac{c\sqrt{2}(\beta c\tau + 6\beta + 2c)\sqrt{q_0}}{6} + q_0\beta^2\tau + 2q_0\beta + \frac{c(c^2 - 2q_0)}{3}\right) \\
& M\left(\frac{14\beta\sqrt{q_0} + \sqrt{2}(c^2 - 2q_0)}{8\beta\sqrt{q_0}}; \frac{5}{2}; \frac{\sqrt{2}\sqrt{q_0}}{\beta}\right) \beta \\
& M\left(\frac{2\beta\sqrt{q_0} + \sqrt{2}(c^2 - 2q_0)}{8\beta\sqrt{q_0}}; \frac{1}{2}; \frac{\sqrt{2}\sqrt{q_0}(\beta\tau + 2)^2}{4\beta}\right) \\
& \left[6\left((\beta\tau + 2)\left(\beta M\left(\frac{2\beta\sqrt{q_0} + \sqrt{2}(c^2 - 2q_0)}{8\beta\sqrt{q_0}}; \frac{1}{2}; \frac{\sqrt{2}\sqrt{q_0}}{\beta}\right)(\sqrt{2}\sqrt{q_0} + c - T_i)\right.\right. \right. \\
& \left. \left. - (\beta\sqrt{2}\sqrt{q_0} + c^2 - 2q_0) M\left(\frac{10\beta\sqrt{q_0} + \sqrt{2}(c^2 - 2q_0)}{8\beta\sqrt{q_0}}; \frac{3}{2}; \frac{\sqrt{2}\sqrt{q_0}}{\beta}\right)\right)\right) \\
& M\left(\frac{6\beta\sqrt{q_0} + \sqrt{2}(c^2 - 2q_0)}{8\beta\sqrt{q_0}}; \frac{3}{2}; \frac{\sqrt{2}\sqrt{q_0}(\beta\tau + 2)^2}{4\beta}\right) + 2\left(\beta\left(-\sqrt{2}\sqrt{q_0} + \beta - c\right.\right. \\
& \left. \left. + T_i\right) M\left(\frac{6\beta\sqrt{q_0} + \sqrt{2}(c^2 - 2q_0)}{8\beta\sqrt{q_0}}; \frac{3}{2}; \frac{\sqrt{2}\sqrt{q_0}}{\beta}\right) + \right. \\
& \left. M\left(\frac{14\beta\sqrt{q_0} + \sqrt{2}(c^2 - 2q_0)}{8\beta\sqrt{q_0}}; \frac{5}{2}; \frac{\sqrt{2}\sqrt{q_0}}{\beta}\right)\left(\beta\sqrt{2}\sqrt{q_0} + \frac{c^2}{3} - \frac{2q_0}{3}\right)\right) \\
& (A.2) \\
& M\left(\frac{2\beta\sqrt{q_0} + \sqrt{2}(c^2 - 2q_0)}{8\beta\sqrt{q_0}}; \frac{1}{2}; \frac{\sqrt{2}\sqrt{q_0}(\beta\tau + 2)^2}{4\beta}\right) \beta \Big]^{-1}.
\end{aligned}$$

Then the functions determining the implicit function curves $\beta_0(c)$ and $\beta_1(c)$ are read as $T(-\ell') - T_0(c) = 0$ and $T(-\ell') - T_1(c) = 0$, respectively:

$$T(-\ell') - T_0(c) = \left[-3\beta\sqrt{c^2 - 2q_0} \left(-\sqrt{2}\sqrt{q_0} + \beta - c + T_i\right)\right]$$

$$\begin{aligned}
& M \left(\frac{6\beta\sqrt{q_0} + (c^2 - 2q_0)\sqrt{2}}{8\beta\sqrt{q_0}}; \frac{3}{2}; \frac{\sqrt{2}\sqrt{q_0}}{\beta} \right) - 3 \left(\beta\sqrt{2}\sqrt{q_0} + \frac{c^2}{3} - \frac{2q_0}{3} \right) \\
& M \left(\frac{14\beta\sqrt{q_0} + (c^2 - 2q_0)\sqrt{2}}{8\beta\sqrt{q_0}}; \frac{5}{2}; \frac{\sqrt{2}\sqrt{q_0}}{\beta} \right) \sqrt{c^2 - 2q_0} + 3\beta \left(-\beta \left(\sqrt{2}\sqrt{q_0} \right. \right. \\
& \left. \left. + c - T_i \right) M \left(\frac{2\beta\sqrt{q_0} + (c^2 - 2q_0)\sqrt{2}}{8\beta\sqrt{q_0}}; \frac{1}{2}; \frac{\sqrt{2}\sqrt{q_0}}{\beta} \right) \right. \\
& \left. \left. + M \left(\frac{10\beta\sqrt{q_0} + (c^2 - 2q_0)\sqrt{2}}{8\beta\sqrt{q_0}}; \frac{3}{2}; \frac{\sqrt{2}\sqrt{q_0}}{\beta} \right) \left(\beta\sqrt{2}\sqrt{q_0} + c^2 - 2q_0 \right) \right) \right] \\
& \left[3\beta \left(-\sqrt{2}\sqrt{q_0} + \beta - c + T_i \right) M \left(\frac{6\beta\sqrt{q_0} + \sqrt{2}(c^2 - 2q_0)}{8\beta\sqrt{q_0}}; \frac{3}{2}; \frac{\sqrt{2}\sqrt{q_0}}{\beta} \right) \right. \\
& \left. + 3M \left(\frac{14\beta\sqrt{q_0} + \sqrt{2}(c^2 - 2q_0)}{8\beta\sqrt{q_0}}; \frac{5}{2}; \frac{\sqrt{2}\sqrt{q_0}}{\beta} \right) \left(\beta\sqrt{q_0}\sqrt{2} + \frac{c^2}{3} - \frac{2q_0}{3} \right) \right]^{-1}, \tag{A.3}
\end{aligned}$$

$$\begin{aligned}
T(-\ell') - T_1(c) &= \left[3\beta\sqrt{c^2 - 2q_0} \left(-\sqrt{2}\sqrt{q_0} + \beta - c + T_i \right) \right. \\
& M \left(\frac{6\beta\sqrt{q_0} + \sqrt{2}(c^2 - 2q_0)}{8\beta\sqrt{q_0}}; \frac{3}{2}; \frac{\sqrt{2}\sqrt{q_0}}{\beta} \right) + 3 \left(\beta\sqrt{q_0}\sqrt{2} + \frac{c^2}{3} - \frac{2q_0}{3} \right) \\
& M \left(\frac{14\beta\sqrt{q_0} + \sqrt{2}(c^2 - 2q_0)}{8\beta\sqrt{q_0}}; \frac{5}{2}; \frac{\sqrt{2}\sqrt{q_0}}{\beta} \right) \sqrt{c^2 - 2q_0} + 3\beta \left(-\beta \left(\sqrt{2}\sqrt{q_0} \right. \right. \\
& \left. \left. + c - T_i \right) M \left(\frac{2\beta\sqrt{q_0} + \sqrt{2}(c^2 - 2q_0)}{8\beta\sqrt{q_0}}; \frac{1}{2}; \frac{\sqrt{2}\sqrt{q_0}}{\beta} \right) \right. \\
& \left. \left. + M \left(\frac{10\beta\sqrt{q_0} + \sqrt{2}(c^2 - 2q_0)}{8\beta\sqrt{q_0}}; \frac{3}{2}; \frac{\sqrt{2}\sqrt{q_0}}{\beta} \right) \left(\beta\sqrt{q_0}\sqrt{2} + c^2 - 2q_0 \right) \right) \right] \\
& \left[3\beta \left(-\sqrt{2}\sqrt{q_0} + \beta - c + T_i \right) M \left(\frac{6\beta\sqrt{q_0} + \sqrt{2}(c^2 - 2q_0)}{8\beta\sqrt{q_0}}; \frac{3}{2}; \frac{\sqrt{2}\sqrt{q_0}}{\beta} \right) \right. \\
& \left. + 3M \left(\frac{14\beta\sqrt{q_0} + \sqrt{2}(c^2 - 2q_0)}{8\beta\sqrt{q_0}}; \frac{5}{2}; \frac{\sqrt{2}\sqrt{q_0}}{\beta} \right) \left(\beta\sqrt{q_0}\sqrt{2} + \frac{c^2}{3} - \frac{2q_0}{3} \right) \right]^{-1}. \tag{A.4}
\end{aligned}$$

APPENDIX B. NUMERICAL SHOOTING METHOD FOR THE ARRHENIUS FUNCTION

In this appendix, we give a discrete method that can be combined with the qualitative results to simulate the bifurcation diagram for the Arrhenius law. To facilitate the use of the Runge-Kutta method for vector field $-\tilde{X}^U$, we take the initial condition $(U(0), T(0)) = (0, T_0(c))$ or $(U(0), T(0)) = (0, T_1(c))$, the final condition $((U(\ell'), T(\ell')) = (\frac{1}{1-\alpha}, T_i)$. In the previous section, where we showed that for the fixed $c_1 \in [c^{ej}, +\infty]$, the transition map $Z(T_0(c_1), \beta, c_1)$ is a monotone continuously increasing function with respect to β (see Proposition 3.9), furthermore, as $\beta \rightarrow +\infty$, $Z(T_0(c_1), \beta, c_1) \rightarrow +\infty$; $Z(T_0(c_1), \beta, c_1) < 1$ when $\beta > 0$ is small enough (see

Proposition 3.4 and Proposition 3.2). Consequently, by continuity and monotonicity, there exists a unique value $\beta = \beta_0(c_1) \in (0, +\infty)$ such that $\mathcal{Z}(T_0(c_1), \beta, c_1) = 1$. The corresponding ℓ' of each pair of parameters (β, c) is finite, has the estimate

$$(B.1) \quad \frac{1}{\beta \exp(-\frac{T_a}{2T_0(c)})} \leq \ell' \leq \frac{1}{\beta \exp(-\frac{T_a}{T_i})}.$$

To illustrate the numerical method, we consider the computation of the curve $\beta_0(c)$. The procedure involves discretizing the parameter space and determining $\beta_0(c)$ for each fixed c . The steps are as follows:

- (1) We restrict the computational region to $(\beta, c) \in [\beta^{low}, \beta^{up}] \times [c^{cj}, c^{up}]$, with $c^{up} > c^{cj}$, $\beta^{up} > \beta^{low} > 0$.
- (2) We discretize the parameter space with uniform meshes: the interval $[c^{cj}, c^{up}]$ with step size $h_c > 0$ and $[\beta^{low}, \beta^{up}]$ with step size $h_\beta > 0$. The resulting grid points are given by:

$$(B.2) \quad (\beta_j, c_i) = (\beta^{low} + jh_\beta, c^{cj} + ih_c),$$

where $i = 0, 1, \dots, N_c$, $j = 0, 1, \dots, N_\beta$, with $N_c = \frac{c^{up} - c^{cj}}{h_c}$ and $N_\beta = \frac{\beta^{up} - \beta^{low}}{h_\beta}$.

- (3) For each fixed c_i , we solve system $-\tilde{X}^U$ for all values of β_j using the 4/5th order Runge-Kutta method. The integration is performed over $[0, \frac{1}{K\beta \exp(-\frac{T_a}{T_i})}]$, with initial conditions $(T(0), U(0)) = (T_0(c_i), 0)$. The numerical step size $d_{(\beta_j, c_i)}$, the temporal mesh points are given by:

$$(B.3) \quad \tau_k = kd_{(\beta_j, c_i)}, \quad k = 0, 1, \dots, N_{ij},$$

where $N_{ij} = \frac{1}{Kd_{(\beta_j, c_i)}\beta \exp(-\frac{T_a}{T_i})}$.

- (4) For each fixed c_i and β_j , we take $\bar{\ell}'(\beta_j, c_i) = \tau_s > 0$ as an approximation of $\ell'(\beta, c)$ such that:

$$(B.4) \quad |U(\bar{\ell}'(\beta_j, c_i), \beta_j, c_i) - \frac{1}{1-\alpha}| = |U(\tau_s, \beta_j, c_i) - \frac{1}{1-\alpha}| = \min_{\tau_k} |U(\tau_k, \beta_j, c_i) - \frac{1}{1-\alpha}|.$$

- (5) For each c_i , we determine $\beta_0(c_i) = \beta_r > 0$ such that:

$$(B.5) \quad |T(\bar{\ell}'(\beta_0(c_i), c_i), \beta_0(c_i), c_i) - T_i| = |T(\bar{\ell}'(\beta_r, c_i), \beta_r, c_i) - T_i| = \min_{\beta_j} |T(\bar{\ell}'(\beta_j, c_i), \beta_j, c_i) - T_i|.$$

- (6) The bifurcation curve $\beta_0(c)$ is visualized by plotting the discrete data points $(\beta_0(c_i), c_i)$, where $i = 0, 1, \dots, N_c$ with $N_c = \frac{c^{up} - c^{cj}}{h_c}$ in the parameter space.

Following the numerical procedure described for $\beta_0(c)$, we can similarly obtain the bifurcation curve $\beta_1(c)$ by replacing $(U(0), T(0)) = (T_1(c), 0)$ with the $(U(0), T(0)) = (T_0(c), 0)$.

The numerical computations are performed with the following specifications:

- MATLAB's ODE solver ODE45 with relative tolerance $\text{RelTol} = 10^{-19}$ and absolute tolerance $\text{AbsTol} = 10^{-22}$;
- Discretization steps: $h_c = 0.02$, $h_\beta = 0.006$;
- Parameter bounds: $[\beta^{low}, \beta^{up}] \times [c^{cj}, c^{up}] = [0.01, 9] \times [0, 9]$.

Here, we remark that the integer index N_{ij} is well defined because the adaptive time-stepping algorithm dynamically adjusts $d_{(c_i, \beta_j)}$ to meet the specified error tolerances while preserving the discretization of the fixed time domain.

Finally, note that to obtain a numerical simulation of the bifurcation curves $\beta_0(c)$ and $\beta_1(c)$ in suitable area, it may be necessary to adjust the parameter ranges $[c^{cj}, c^{up}]$ and $[\beta^{low}, \beta^{up}]$ according to the specific behavior of the system.

(C.-M. Brauner) INSTITUT DE MATHÉMATIQUES DE BORDEAUX UMR CNRS 5251, UNIVERSITÉ DE BORDEAUX, 33405 TALENCE, FRANCE

Email address: `claude-michel.brauner@u-bordeaux.fr`

(J. Jing) SCHOOL OF MATHEMATICS AND STATISTICS, YUNNAN UNIVERSITY, KUNMING, 615000, CHINA

Email address: `jingjinlong@stu.ynu.edu.cn`

(R. Roussarie) IMB UMR 5584, UNIVERSITÉ DE BOURGOGNE EUROPE, CNRS, F-21000 DIJON, FRANCE

Email address: `Robert.Roussarie@u-bourgogne.fr`